Development 135, 95-109 (2008) doi:10.1242/dev.011072

Matrix metalloproteinases promote motor axon fasciculation in the *Drosophila* embryo

Crystal M. Miller[1], Andrea Page-McCaw[2] and Heather T. Broihier[1,*]

Matrix metalloproteinases (MMPs) are a large conserved family of extracellular proteases, a number of which are expressed during neuronal development and upregulated in nervous system diseases. Primarily on the basis of studies using pharmaceutical inhibitors, MMPs have been proposed to degrade the extracellular matrix to allow growth cone advance during development and hence play largely permissive roles in axon extension. Here we show that MMPs are not required for axon extension in the *Drosophila* embryo, but rather are specifically required for the execution of several stereotyped motor axon pathfinding decisions. The *Drosophila* genome contains only two MMP homologs, *Mmp1* and *Mmp2*. We isolated *Mmp1* in a misexpression screen to identify molecules required for motoneuron development. Misexpression of either MMP inhibits the regulated separation/defasciculation of motor axons at defined choice points. Conversely, motor nerves in *Mmp1* and *Mmp2* single mutants and *Mmp1 Mmp2* double mutant embryos are loosely bundled/fasciculated, with ectopic axonal projections. Quantification of these phenotypes reveals that the genetic requirement for *Mmp1* and *Mmp2* is distinct in different nerve branches, although generally *Mmp2* plays the predominant role in pathfinding. Using both an endogenous MMP inhibitor and MMP dominant-negative constructs, we demonstrate that MMP catalytic activity is required for motor axon fasciculation. In support of the model that MMPs promote fasciculation, we find that the defasciculation observed when MMP activity is compromised is suppressed by otherwise elevating interaxonal adhesion – either by overexpressing *Fas2* or by reducing *Sema-1a* dosage. These data demonstrate that MMP activity is essential for embryonic motor axon fasciculation.

KEY WORDS: *Drosophila melanogaster*, Motoneuron, Motor axon pathfinding, Mmp1, Mmp2, Sema-1a, Fasciclin II, Timp

INTRODUCTION

Motor axons navigate an extracellular environment rich with potentially competing attractive and repulsive cues. Remarkably, motor axon growth cones are able to both interpret and integrate the signals present in this complex environment en route to their individual muscle targets. The particular axonal trajectory taken by any given motoneuron depends on the nature of the extracellular cues encountered by the extending axon as well as the complement of receptor or adhesion molecules expressed on its growth cone. In addition, several molecules required for either the activation or distribution of extracellular guidance molecules have recently been implicated in axon guidance (Johnson et al., 2004; Meyer and Aberle, 2006; Parker et al., 2006; Serpe and O'Connor, 2006; Steigemann et al., 2004).

The number and diversity of molecules implicated in motor axon pathfinding suggest that work in genetic model systems will continue to be essential to identify and tease apart the relative contributions of proteins involved in this process. In particular, the *Drosophila* embryo provides an important model for the study of motor axon pathfinding as a result of the small number of motoneurons, their defined trajectories and invariant muscle targets (Landgraf et al., 1997; Schmid et al., 1999; Sink and Whitington, 1991). Work by a number of groups has led to the identification and characterization of molecules critical for pathfinding and target recognition by *Drosophila* motor axons (Fox and Zinn, 2005; Terman et al., 2002; Van Vactor et al., 1993). An underlying principle to emerge from these studies is that in order for axons to reach their muscle targets, the activity of adhesion molecules that promote the fasciculation and/or bundling of motor axons must be precisely balanced with repulsive signals that trigger the defasciculation and/or separation of the extending axons (Winberg et al., 1998a; Yu et al., 2000).

Although the mechanisms responsible for limiting defasciculation to defined choice points in the periphery are not clear, a number of molecules necessary for proper defasciculation have been identified. In particular, repulsive signaling mediated by the Semaphorin-Plexin (Sema-Plex) pathway is essential for motor axon defasciculation (Ayoob et al., 2006; Terman et al., 2002; Winberg et al., 1998a; Yu et al., 2000). In wild-type embryos, axons of the intersegmental nerve branch b (ISNb) defasciculate from the primary ISN pathway and innervate the ventrolateral muscle (VLM) field. In embryos with reduced Sema-Plex pathway activity, however, ISNb axons fail to reach their targets and often remain bundled with the primary ISN branch – a phenotype consistent with diminished interaxonal repulsion. Furthermore, embryos with loss-of-function (LOF) mutations in *nervy* and *protein kinase A RII*, two genes that have been proposed to antagonize Sema-Plex signaling, exhibit premature and excessive motor axon defasciculation (Terman and Kolodkin, 2004). By contrast, LOF mutations in the genes for cell adhesion molecules Fasciclin II (FasII) or Connectin (Con) suppress LOF mutations in *Sema-1a* and *plexA*, arguing that Sema-1a and PlexA stimulate defasciculation by overcoming axon-axon adhesion maintained by FasII and Con (Winberg et al., 1998a; Yu et al., 2000). These genetic interaction studies demonstrate the importance of balancing attractive and repulsive forces to enable correct fasciculation and pathfinding.

[1]Department of Neurosciences, Case Western Reserve University School of Medicine, 10900 Euclid Avenue, Cleveland, OH 44106, USA. [2]Department of Biology and Center for Biotechnology and Interdisciplinary Studies, Rensselaer Polytechnic Institute, 110 8th Street, Troy, NY 12180, USA.

*Author for correspondence (e-mail: heather.broihier@case.edu)

Accepted 6 October 2007

To understand how the precise balance of attraction and repulsion is achieved, the roles of additional molecules capable of modulating fasciculation of extending motor axons must be characterized. A number of studies have investigated the roles of metalloproteinases in axon extension and guidance. The metzincin metalloproteinases are zinc-dependent extracellular proteases that are subdivided into four subfamilies based on structure: astacins, serralysins, matrix metalloproteinases (MMPs) and adamlysins – a subfamily that includes the ADAMs (a disintegrin and a metalloproteinase) (Sternlicht and Werb, 2001). Classic models of metalloproteinase function in neuronal development proposed that they acted to degrade extracellular matrix (ECM) in order to clear a path for advancing axons (Muir, 1994; Zuo et al., 1998). Recently, the roles of metalloproteinases in axonogenesis have been revisited in a number of experimental systems (McFarlane, 2003). These studies indicate that relevant neuronal metalloproteinase substrates include molecules directly involved in mediating axon pathfinding, including guidance receptors and their ligands. Among the metalloproteinases, the ADAM family is most strongly implicated in the regulation of axon guidance. For instance, ADAM10 terminates the interaction between ephrin A2 and EphA by cleaving ephrin A2, thereby facilitating axon retraction in vitro (Hattori et al., 2000). Analyses of *Drosophila* embryos mutant for the ADAM family homolog *kuzbanian* (*kuz*) further support the idea that ADAMs regulate particular guidance events, as *kuz* mutations display genetic interactions with mutations in the repulsive midline factor *slit* (Schimmelpfeng et al., 2001). Interestingly, independent work from several groups has recently provided evidence that *tolloid-related 1* (*tlr1*; also known as *tolkin* – FlyBase), a *Drosophila* astacin-family metalloproteinase, acts through its TGFβ ligand Dawdle to regulate motor axon guidance in the embryo (Meyer and Aberle, 2006; Parker et al., 2006; Serpe and O'Connor, 2006).

As a family, MMPs are able to cleave nearly every component of the ECM, as well as numerous signaling molecules and cell surface receptors (Sternlicht and Werb, 2001). In the CNS, investigations of MMP function have largely centered on the roles of these proteases in nervous system disease, as MMPs are known to be dramatically upregulated in a host of CNS diseases, as well as following nervous system injury (Yong, 2005; Yong et al., 2001). However, in large part due to issues of redundancy and compensation among the twenty-four vertebrate MMP family members, the normal physiological roles of MMPs in the nervous system have remained largely elusive. Notably, a number of vertebrate MMPs display neuronal expression patterns in the embryo, suggesting that they may be involved in normal nervous system development (Gonthier et al., 2007; Hayashita-Kinoh et al., 2001; Hehr et al., 2005). In support of this model, studies of *Xenopus* retinal ganglion cell axon guidance using MMP pharmaceutical inhibitors suggest that MMPs are required for specific pathfinding decisions (Hehr et al., 2005). *Drosophila* affords an attractive genetic model system in which to study MMP function since there are only two MMP family members in the fly, *Mmp1* and *Mmp2* (Llano et al., 2002; Llano et al., 2000; Page-McCaw et al., 2003). Whereas Mmp1 is a secreted protein, Mmp2 contains a GPI-anchor sequence and has been shown to be membrane-bound in tissue culture cells.

In this work, we present an analysis of MMP function during *Drosophila* embryonic neuronal development. Both LOF and gain-of-function (GOF) analyses support the model that MMP activity promotes motor axon fasciculation in the embryo. Misexpression of either *Mmp1* or *Mmp2* drives excessive motor axon fasciculation. By contrast, we find aberrant defasciculation in MMP LOF mutants. Although *Mmp1* mutants display relatively mild pathfinding defects, many motor axons separate prematurely and aberrantly in *Mmp2* single mutants and *Mmp1 Mmp2* double mutants, indicating that *Mmp2* plays a primary role in motor axon fasciculation. We have analyzed the embryonic expression of both MMPs and find that whereas *Mmp1* exhibits a limited embryonic expression profile, *Mmp2* is expressed in neurons and glia – supporting a primary role for *Mmp2* in embryonic neuronal development. Importantly, we find aberrant motor axon defasciculation in embryos misexpressing the endogenous MMP inhibitor *Timp* and in embryos misexpressing MMP dominant-negative constructs, indicating that MMP catalytic activity is essential for pathfinding. Finally, we show that the defasciculation phenotype exhibited by MMP LOF mutants are dominantly suppressed by LOF mutations in *Sema-1a*, arguing that MMP activity normally acts to promote fasciculation by antagonizing *Sema-1a* function. Together, our results indicate that MMPs are not required for motor axon extension per se, but instead may modulate the responses of the axons of defined neuronal populations to specific guidance cues.

MATERIALS AND METHODS

Gene misexpression screen

To identify novel factors required for embryonic CNS development, we conducted a GOF screen for genes whose misexpression disrupted motoneuron fate or pathfinding. We screened a collection of 2800 *Drosophila* lines harboring P elements containing the yeast GAL4 binding site UAS (Rorth et al., 1998; Toba et al., 1999; Viquez et al., 2006). Males from these P-element insertion lines were crossed to *elavGAL4* virgin females to drive misexpression of the gene adjacent to the P-element insertion in all post-mitotic neurons (DiAntonio et al., 2001; Yao and White, 1994). We first selected those lines in which *elavGAL4*-dependent misexpression was lethal, as we reasoned this would enrich for genes with neuronal misexpression phenotypes. As a secondary screen, we crossed males from the 114 *elavGAL4*-dependent lethal lines to *elavGAL4* virgins and collected embryos to screen for neuronal phenotypes. We analyzed CNS cell fate by staining with antibodies labeling specific neuronal populations, including anti-Even-skipped, anti-Hb9 [also known as Extra-extra (Exex) – FlyBase], and anti-Nkx6 (also known as HGTX – FlyBase) (Broihier et al., 2004; Broihier and Skeath, 2002; Landgraf et al., 1999). For lines in which neuronal fate appeared normal, we screened for motor axon guidance phenotypes using anti-Fasciclin II (anti-FasII) (Van Vactor et al., 1993) to label motor axon projections.

Fly stocks

Stocks used in this work include: $Mmp2^{W307*}$, $Mmp2^{Df(2R)Uba1\text{-}Mmp2}$, $Mmp1^{Q112*}$, $Mmp1^{2}$, $Mmp2^{W307*}$ $Mmp1^{Q112*}$, $Mmp2^{Df(2R)Uba1\text{-}Mmp2}$ $Mmp1^{2}$, *UAS-TIMP*, *UAS-Mmp2*, *UAS-Mmp1* (Page-McCaw et al., 2003), *UAS-*$Mmp2^{E258A}$ (below), *UAS-*$Mmp1^{E225A}$ (Zhang et al., 2006), *UAS-Fas2* from A. Kolodkin (Johns Hopkins University, Baltimore, MD), *elavGAL4* from A. DiAntonio (Washington University, St Louis, MO), $gcm^{\Delta P1}$ from M. Freeman (University of Massachusetts, Worcester, MA), *repoGAL4* from J. Simpson (HHMI Janelia Farm Research Campus, Ashburn, VA), $Hb9^{GAL4}$ (Broihier and Skeath, 2002). The $Sema\text{-}1a^{P1}$ $Mmp2^{W307*}$, $Sema\text{-}1a^{P1}$ $Mmp1^{Q112*}$ recombinant chromosomes were generated by standard genetic techniques. All other stocks were obtained from Bloomington Stock Center.

Transgenic MMP constructs

UAS-$Mmp1^{E225A}$ contains a missense mutation in the conserved catalytic core that renders the enzyme catalytically inactive; in cell culture $Mmp1^{E225A}$ acts dominantly to inhibit Mmp1 function (Zhang et al., 2006). Similarly, *UAS-*$Mmp2^{E258A}$ disrupts the conserved catalytic core of Mmp2 and is expected to function as a dominant negative; the PCR-generated mutant cDNA was cloned into pUAST and injected into flies by standard methods. For the misexpression analysis with *elavGAL4* and *repoGAL4*, similar results were observed with each of two independent transgenic lines for both

UAS-Mmp1 and *UAS-Mmp2* (Page-McCaw et al., 2003). This similarity argues that the observed phenotypic differences are unlikely to be the result of expression level differences between the UAS responder lines.

Antibodies

Drosophila embryos were fixed by gentle rocking for 4 minutes in 2 ml heptane and 2 ml 37% formaldehyde followed by 30 seconds of shaking in 6 ml methanol to devitellinize. The following primary antibodies were used: mouse anti-FasII/1D4 at 1:10 [generated by C. Goodman and obtained from the Developmental Studies Hybridoma Bank (DSHB)], rabbit anti-GFP at 1:100 (Invitrogen), mouse anti-Wrapper at 1:10 (generated by C. Goodman and obtained from the DSHB), mouse anti-Repo at 1:10 (generated by C. Goodman and obtained from the DSHB), mouse anti-β-gal at 1:1000 (Promega), rat anti-Islet at 1:100 and rabbit anti-Hb9 at 1:500 (Broihier and Skeath, 2002), and an anti-Mmp1 monoclonal cocktail (a 1:1:1 mixture of 3B8, 5H7 and 23G1) at 1:50 (generated by A. Page-McCaw and obtained from the DSHB). Species-specific biotinylated secondary antibodies were used at 1:300 in concert with the ABC Elite kit for immunohistochemistry (Vector Labs). Species-specific Alexa Fluor 488 and Alexa Fluor 568 (Molecular Probes) were used for immunofluorescence. Embryos stained with anti-GFP were fixed for 40 minutes in 3 ml heptane and 3 ml 4% paraformaldehyde. For these embryos, incubation with ABC was followed by treatment with the TSA Biotin System kit (PerkinElmer), followed by another incubation with ABC before developing.

In situ hybridization

An antisense digoxigenin-labeled *Mmp2* RNA probe was generated with T7 polymerase from a full-length cDNA. Sense probes generated with T3 polymerase did not result in specific hybridization. Embryos were incubated with riboprobe at 57°C overnight. RNA probe hybridization was visualized with an alkaline phosphatase-conjugated anti-DIG antibody (Roche) followed by NBT and BCIP treatment. For double labeling with in situ probe and antibody, the in situ hybridization protocol was followed by storage in 70% ethanol overnight and standard antibody staining. For fluorescent labeling, an anti-DIG-POD antibody (Roche) was used to recognize the probe and was amplified using the TSA Plus Fluorescence system (PerkinElmer).

Microscopy and data analysis

Embryos were filleted in 70% glycerol under a Leica MZ125 dissecting microscope. Specimens were analyzed on a Zeiss Axioplan 2 microscope with a 63× or 100× oil-immersion objective using Nomarski optics, and images were captured with an AxioCam MRc camera. Brightness and contrast were adjusted using Adobe Photoshop. Fluorescence images were obtained on a Zeiss Axio Imager.Z1 confocal microscope and edited with LSM 5 Image Browser. Statistical analyses were performed using Fisher's exact test.

RESULTS

Pan-neuronal misexpression of either *Mmp1* or *Mmp2* inhibits motor axon defasciculation

We conducted a misexpression screen to identify genes required for embryonic neuronal fate and axon pathfinding (see Materials and methods). In this manner, we identified several P-element lines in which the wild-type pattern of motor axon projections was disrupted. In wild type, ISNb axons defasciculate or separate from the primary ISN nerve at their first choice point proximal to the ventrolateral muscle (VLM) field. Within the VLM field, ISNb axons continue to extend dorsally, with axonal subsets defasciculating from the ISNb at secondary choice points when they contact their muscle targets (Fig. 1A,D). Embryos from one of the lines isolated in the screen, GS2402, exhibited strongly stalled ISNb motor axons (termed a 'stall' phenotype; data not shown). Inverse PCR analysis indicated that this line contained a P element inserted directly upstream of *Mmp1*.

To confirm that *Mmp1* misexpression was responsible for the motor axon phenotypes observed in GS2402, we used a *UAS-Mmp1* transgene (Page-McCaw et al., 2003) to drive *Mmp1* throughout the embryonic CNS via *elavGAL4*. Consistent with the identification of *Mmp1* in our screen, neuronal misexpression of *Mmp1* interferes with embryonic motor axon guidance (Table 1; Fig. 1A,B). ISNb morphology was disrupted in *elavGAL4/UASMmp1* mutant embryos in 74% of hemisegments scored (n=138). The majority of affected hemisegments displayed phenotypes indicative of increased motor axon fasciculation, ranging from relatively mild defects to a complete block of proper ISNb defasciculation. Specifically, aberrant hemisegments often exhibited ISNb stall phenotypes, in which ISNb axons separated from the ISN at their first choice point, but subsequently failed to defasciculate from each other at their individual muscle targets, instead stalling in the ventral longitudinal muscle field (33%; Table 1; Fig. 1B,E). In 14% of hemisegments we observed a stronger 'fusion bypass' phenotype, in which ISNb axons failed to defasciculate from the ISN at the first ISNb choice point and remained bundled with ISN axons (e.g. Fig. 3C).

To investigate whether the effects of *Mmp1* misexpression were restricted to the ISNb branch, we evaluated segmental nerve branch a (SNa) guidance in embryos with *Mmp1* expressed pan-neuronally. In wild type, axons within SNa exit the CNS and extend dorsally past the ventral longitudinal muscles to innervate the lateral muscle

Table 1. *MMP/Timp* misexpression phenotypes

Genotype	Total aberrant ISNb* % (n)	Total hyperfasciculation ISNb %			Hypofasciculation ISNb %	Total aberrant SNa % (n)	Hyperfasciculation SNa %	Hypofasciculation SNa %
		Stall	Fusion bypass	Total				
Wild type	13 (140)	7	0	7	6	11 (160)	5	7
elav>Mmp1	74 (138)	33	14	47	11	50 (129)	39	11
repo>Mmp1	46 (121)	17	9	26	16	68 (131)	44	24
elav>Mmp2	72 (147)	39	11	50	1	80 (145)	68	12
repo>Mmp2	82 (120)	33	30	63	3	70 (109)	61	9
elav>Timp	54 (425)	7	1	8	41	58 (439)	17	44
repo>Timp	65 (362)	4	0	4	54	75 (357)	24	54
elav>Mmp2^{E258A}	66 (167)	13	1	14	37	64 (125)	49	23
repo>Mmp2^{E258A}	72 (141)	4	2	6	50	54 (163)	26	36
elav>Mmp1^{E225A}	58 (147)	1	0	1	34	42 (147)	9	33
repo>Mmp1^{E225A}	61 (150)	3	0	3	39	34 (149)	9	24

n, The number of hemisegments scored for each genotype.
*Includes hyperfasciculated, hypofasciculated and loss/reduction of the synapse in the 6/7 muscle cleft, which could be attributed to either hypo- or hyperfasciculation.

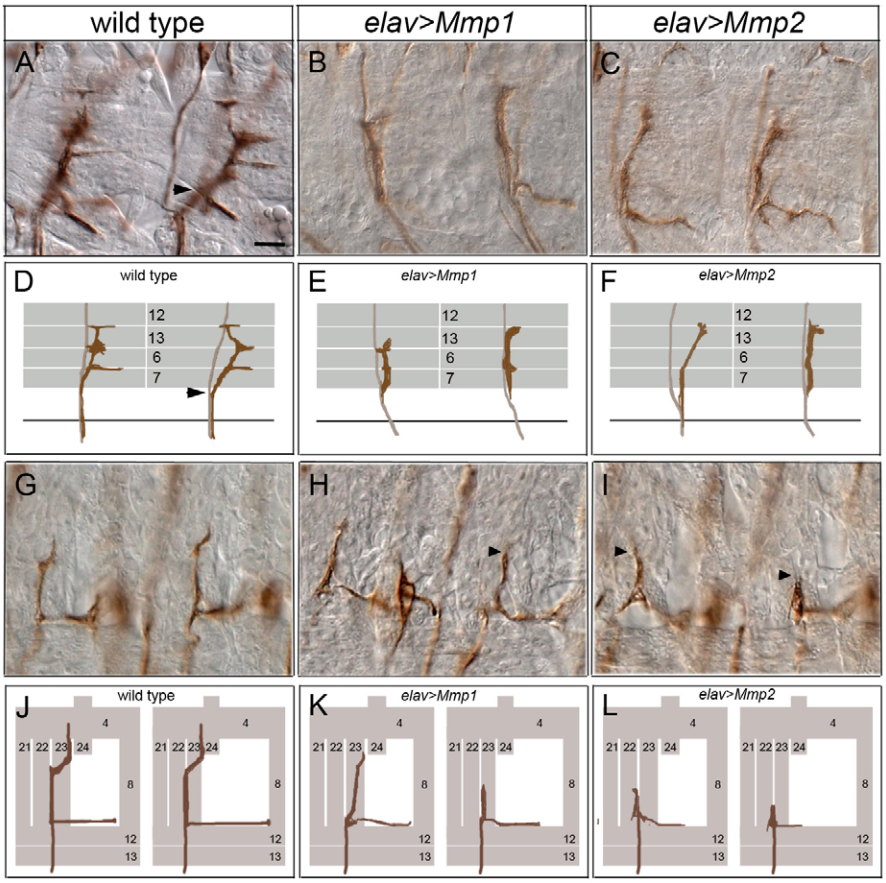

Fig. 1. Pan-neuronal misexpression of either *Mmp1* or *Mmp2* inhibits motor axon defasciculation. In each micrograph, two abdominal hemisegments of stage 17 dissected embryos stained with α-FasII to label the motor projections are shown with anterior left and dorsal up. Below each image are schematics diagramming the observed phenotypes with motor axons in brown and muscles represented by gray boxes. In all ISNb schematics, the muscles are drawn as if transparent in order to depict both the ISN and ISNb pathways. However, note that the ISN extends in an external plane whereas the ISNb extends in an internal plane. (**A**,**D**) In wild type, ISNb axons defasciculate from the ISN at a choice point proximal to the VLM field (arrowheads), then continue to extend dorsally to innervate muscles 7, 6, 13, 12. (**B**,**C**,**E**,**F**) In *elav>Mmp1* and *elav>Mmp2* embryos, ISNb axons appear to defasciculate correctly from the ISN at their first choice point, but fail to defasciculate at their appropriate muscle targets, a phenotype referred to as 'stall'. (**G**,**J**) In wild type, the SNa branch innervates the lateral musculature and comprises dorsal and posterior branches. The posterior branch extends posteriorly to innervate muscle 8, whereas the dorsal branch makes two stereotyped turns en route to muscles 23 and 24. (**H**,**K**) In *elav>Mmp1* embryos, the dorsal branch of the SNa stalls (arrowhead) before reaching its final target. (**I**,**L**) In *elav>Mmp2* embryos, the dorsal (arrowheads) and lateral branches of the SNa stall before reaching their synaptic targets. Scale bar: 15 μm.

field. Just dorsal to the ventral longitudinal muscles, SNa axons reach their first choice point and separate into dorsal and posterior branches. Axons in the posterior branch innervate muscle 8, whereas axons in the dorsal branch extend dorsally between muscles 22 and 23 before subdividing again at their second choice point with a posterior sub-branch turning to innervate muscle 24 (Fig. 1G,J; Table 1). We found that neuronal misexpression of *Mmp1* disrupted SNa pathfinding in 50% of hemisegments, with most hemisegments (39%) containing SNa nerves that failed to branch appropriately or stalled in the lateral muscle field. Typically, axons in the dorsal SNa branch failed to separate at the second choice point resulting in a failure to innervate muscle 24 (Fig. 1H,K; Table 1). These data demonstrate that neuronal *Mmp1* misexpression drives axon hyperfasciculation in multiple embryonic motor nerve pathways.

Since vertebrate MMPs often display overlapping substrate specificities (Page-McCaw et al., 2007), we wanted to determine whether neuronal misexpression of *Mmp2* would have similar phenotypic consequences to *Mmp1* misexpression. We found that *elavGAL4/UASMmp2* embryos also exhibit aberrant axonal phenotypes consistent with increased motor axon fasciculation (Fig. 1; Table 1). In these embryos, ISNb pathfinding is aberrant in 72% of hemisegments, with 50% of all hemisegments displaying either ISNb stall or fusion bypass phenotypes (n=147; Fig. 1C,F). Furthermore, neuronal misexpression of *Mmp2* interfered with SNa pathfinding in 80% of hemisegments, with axons in 68% of hemisegments either stalling or failing to branch appropriately (Fig. 1I,L). Although *Mmp1* and *Mmp2* misexpression have comparable effects on ISNb pathfinding, SNa appears particularly sensitive to *Mmp2* levels since the penetrance of SNa phenotypes is significantly higher with *Mmp2* misexpression (P<0.0001; Table 1). Together, these data indicate that pan-neuronal misexpression of either MMP inhibits the ability of motor axons in both ISNb and SNa to appropriately defasciculate en route to their muscle targets and raises the possibility that matrix metalloproteinases contribute to proper motor axon guidance in the embryo.

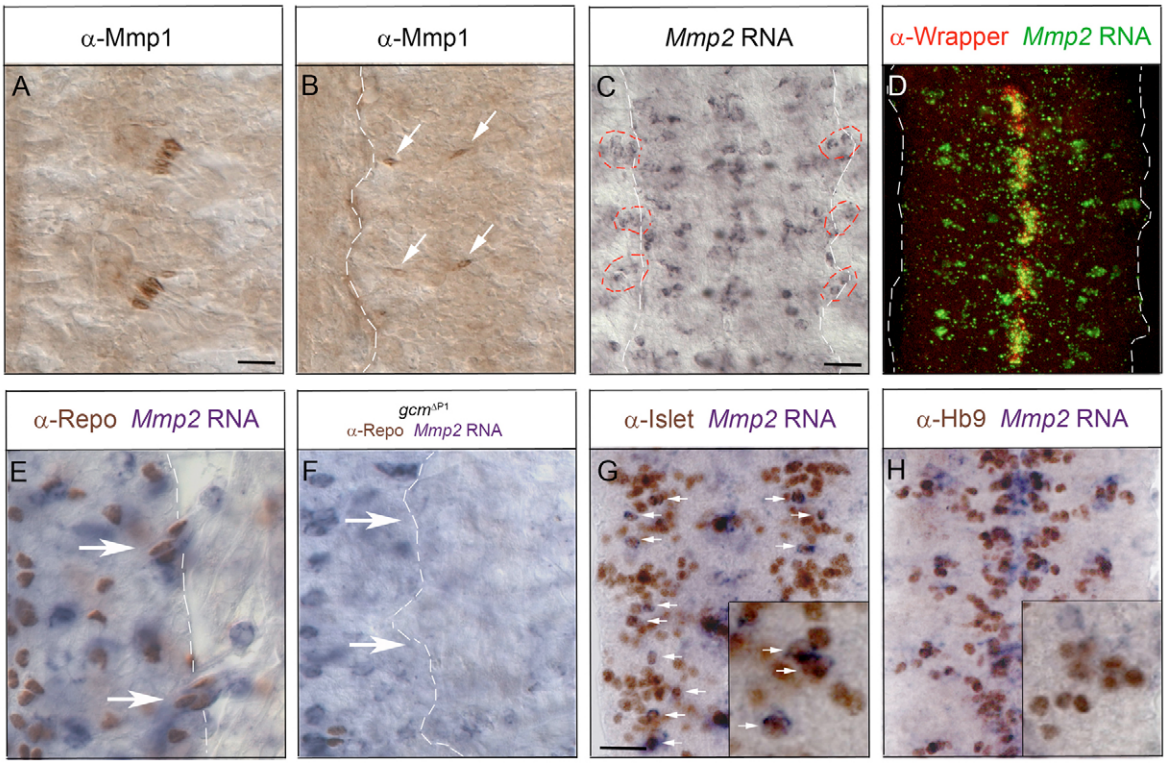

Fig. 2. Embryonic expression profiles of *Mmp1* and *Mmp2*. (**A-E**,**G**,**H**) Stage 15 wild-type embryos stained for indicated markers. (**F**) Stage 15 $gcm^{\Delta P1}$ homozygous mutant embryo stained for *Mmp2* RNA and labeled with anti-Repo. (A) Mmp1 is expressed in PNS neurons in the chordotonal organs and (B) in two cells in the ventral longitudinal muscle field (arrows). (C) Expression of *Mmp2* RNA indicates that *Mmp2* is expressed in a subset of CNS neurons and glia (circled in red). (D) *Mmp2* RNA (green) colocalizes with anti-Wrapper (red) in midline glia. (E) Nuclear anti-Repo (brown) and cytoplasmic *Mmp2* RNA (purple) in a subset of exit glia (arrows). (F) In $gcm^{\Delta P1}$ embryos, which lack most glia, *Mmp2* RNA is no longer expressed at the lateral edge of the CNS where the exit glia are located (arrows). (G) Anti-Islet (brown) colocalizes with *Mmp2* RNA (purple) in approximately three neurons per hemisegment (arrows). The location of these neurons is consistent with an interneuron identity. (H) Anti-Hb9 (brown) does not colocalize with *Mmp2* RNA (purple). Insets in G and H show high-magnification views of *Mmp2* expression. Dotted white line marks the CNS boundary. Anterior is up in all panels. Dorsal is right in A,B,E,F. Scale bars: 10 μm in A,B,E,F; 20 μm in C,D,G,H.

MMPs exhibit distinct and spatially restricted expression profiles in embryogenesis

To further investigate the possibility that MMP activity plays a role in neuronal development, we characterized the embryonic expression patterns of *Mmp1* and *Mmp2*. Previous studies have established that both genes are embryonically expressed (Llano et al., 2002; Llano et al., 2000; Page-McCaw et al., 2003). Using anti-Mmp1 antibodies, we found Mmp1 protein to be expressed in essentially the same spatiotemporal expression profile as has been described for *Mmp1* RNA. The most prominent embryonic expression of Mmp1 is in the proventriculus and hindgut (data not shown). Consistent with previous studies (Llano et al., 2000; Page-McCaw et al., 2003), we found Mmp1 CNS expression to be restricted to small clusters of segmentally repeating cells at the CNS midline (data not shown). We also detected Mmp1 expression in the chordotonal organs of the peripheral nervous system (Fig. 2A) and in two cells situated in the ventral mesodermal region (Fig. 2B). This expression is undetectable in *Mmp1*-null mutant embryos, ($Mmp1^{2}/Mmp1^{Q112*}$), confirming antibody specificity (data not shown).

We next characterized the expression pattern of *Mmp2* via whole-mount RNA in situ hybridization. In contrast to *Mmp1*, *Mmp2* is widely expressed in the embryonic CNS (Fig. 2C). To identify the neuronal cells, we double labeled wild-type embryos with *Mmp2* RNA and markers for specific neural and glial populations. We found that *Mmp2* is expressed in midline glia as *Mmp2* RNA is co-expressed with Wrapper in these cells (Fig. 2D) (Noordermeer et al., 1998). We next tested whether *Mmp2* is expressed in additional glial populations by co-labeling embryos with *Mmp2* RNA and the glial marker anti-Repo (Xiong et al., 1994). At stage 15, *Mmp2* and Repo are co-expressed in approximately three glial cells per hemisegment situated at the base of motor nerve roots (circled cells in Fig. 2C, arrows in Fig. 2E). The position and morphology of these cells suggest they correspond to exit glia, a group of peripheral glia originating within the CNS before migrating into the periphery during embryogenesis along extending motor axons (Klambt and Goodman, 1991; Sepp et al., 2000). To confirm that these Mmp2-expressing cells are glia, we asked whether they are absent in embryos mutant for *glial cells missing* (*gcm*), in which the number of glial cells is greatly reduced (Jones et al., 1995). In support of this conclusion, *gcm* mutant embryos specifically lack the *Mmp2*-expressing cells situated at the boundary between the CNS and periphery (arrows in Fig. 2F).

The observation that *Mmp2*-positive cells within the CNS do not co-express Repo suggested that they are probably neurons. To determine whether they correspond to well-characterized subsets of motoneurons or interneurons, we double labeled embryos with *Mmp2* RNA and antibodies specific for particular neuronal populations. We detected co-expression between *Mmp2* and Islet, a marker for distinct motoneuron and interneuron populations (Thor

and Thomas, 1997), in three neurons per hemisegment in the lateral CNS (arrows in Fig. 2G). We next asked whether these *Mmp2*-expressing neurons are Hb9-positive motoneurons. We did not detect co-expression between Hb9 and *Mmp2* RNA (Fig. 2H), suggesting that the *Mmp2*-positive neurons in the lateral CNS are Islet-positive interneurons. In sum, whereas *Mmp1* exhibits a limited neuronal expression pattern, *Mmp2* is expressed in stereotyped populations of neurons and glia, consistent with a role for *Mmp2* in neuronal development.

MMP misexpression in glia blocks motor axon defasciculation

Mmp1 is a secreted protein, whereas Mmp2 contains a GPI-anchor and is membrane-associated (Llano et al., 2002; Llano et al., 2000; Page-McCaw et al., 2003) – suggesting that the distribution of *Mmp2* may be critical for *Mmp2* to have access to its substrate. Although we did not detect endogenous *Mmp2* RNA expression in the mesoderm or in motoneurons, *Mmp2* is expressed in a subset of peripheral glia that are closely associated with extending motor axons. To test if glial expression of *Mmp2* might play a role in motor axon pathfinding, we analyzed the phenotypic consequences of *Mmp2* misexpression in glia using a *repoGAL4* driver. For comparison, we also quantified motor axon pathfinding in *repoGAL4>Mmp1* embryos. We first visualized glia in *repo>Mmp1* and *repo>Mmp2* embryos with anti-Repo since MMP misexpression might interfere with the migration of peripheral glia along the motor nerves (Sepp et al., 2000) and thereby indirectly influence motor axon pathfinding. We found that the number and position of Repo-positive glia are unaltered with glial misexpression of either *Mmp1* or *Mmp2* (data not shown).

We then analyzed motor axon pathfinding in *repo>MMP* embryos. Glial misexpression of either MMP leads to phenotypes that are qualitatively similar to those observed with neural misexpression. In these embryos, axons in both ISNb and SNa stall prematurely and fail to branch appropriately (Table 1; Fig. 3). For *Mmp1*, the frequency of ISNb hyperfasciculation decreases from 47% in *elav>Mmp1* embryos to 26% in *repo>Mmp1* embryos, suggesting that the level of secreted Mmp1 may be higher with neuronal than with glial misexpression. By contrast, glial misexpression of *Mmp2* significantly increases the frequency of motor axon fasciculation defects compared to neural misexpression of *Mmp2* in the ISNb (63% vs 50%; $P<0.05$; Table 1; Fig. 3C,F). This is particularly striking for the ISNb fusion bypass phenotype – the strongest class of ISNb hyperfasciculation. We observed a fusion bypass phenotype in 11% of hemisegments in *elav>Mmp2* embryos, compared to 30% in *repo>Mmp2* hemisegments (Table 1). Hence, glial misexpression of *Mmp1* does not enhance the phenotypes above those observed with *elavGAL4*; by contrast, *Mmp2* misexpression in glia yields phenotypes significantly stronger than those induced by neuronal misexpression.

Since MMP misexpression in neurons or glia increases motor axon fasciculation, we next wanted to determine whether MMP misexpression in other embryonic tissues is also sufficient to interfere with motor axon pathfinding. Hence, we analyzed motor axon guidance in embryos misexpressing either *Mmp1* or *Mmp2* in mesoderm (using *24B-Gal4* and *dmef2GAL4* drivers) or hemocytes (using *HeGAL4* and *CrqGAL4* drivers). We did not detect motor axon phenotypes in embryos with MMP misexpression using any of these GAL4 drivers (data not shown), indicating that motor axon pathfinding is not affected by MMP misexpression in mesoderm or

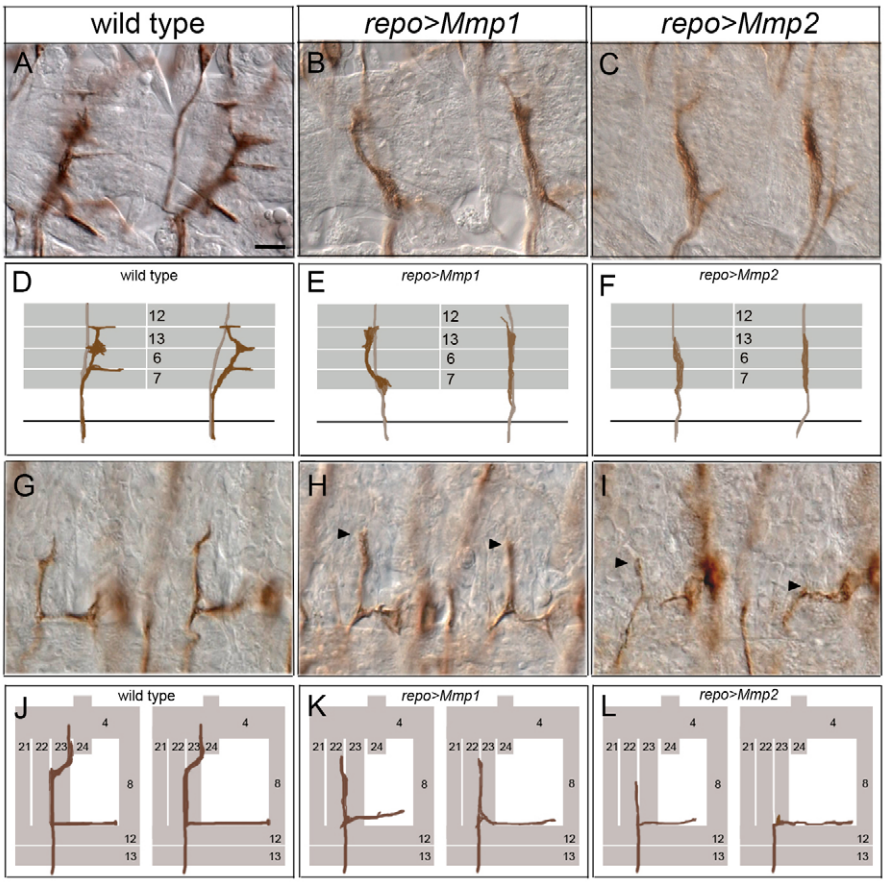

Fig. 3. Pan-glial misexpression of *Mmp1* or *Mmp2* blocks motor axon defasciculation. In each micrograph, two abdominal hemisegments of stage 17 dissected embryos stained with α-FasII to label the motor projections are shown with anterior left and dorsal up. Below each image are schematics of the observed phenotypes with motor axons in brown and muscles represented by gray boxes. (**A**,**D**) In wild type, axons in ISNb defasciculate from the ISN and extend dorsally to their synaptic targets. (**B**,**C**,**E**,**F**) In *repo>Mmp1* and *repo>Mmp2* embryos, ISNb axons fail to defasciculate appropriately and instead remain tightly bundled together, exhibiting either a 'parallel bypass' (B,E); or a stronger 'fusion bypass' phenotype (C,F). In fusion bypass, ISNb axons fail to separate from ISN axons at their first choice point and bypass the VLM field. (**G**,**J**) In wild type, SNa axons bifurcate into dorsal and posterior SNa branches and innervate lateral muscle targets. (**H**,**K**) *repo>Mmp1* embryos exhibit mild stalls of the dorsal SNa branch (arrowheads). (**I**,**L**) *repo>Mmp2* embryos display strongly truncated dorsal branches (arrowheads) and mildly stalled posterior branches. Scale bar: 15 μm.

hemocytes, but is sensitive to elevated MMP levels in neurons and glia. For *Mmp2* in particular, the penetrance and expressivity of motor axon phenotypes observed with glial *Mmp2* misexpression as well as the endogenous expression of *Mmp2* in a subset of peripheral glia suggest that *Mmp2* expression levels in peripheral glia are critical for proper motor axon guidance.

MMP LOF mutants display inappropriate motor axon defasciculation

To determine if MMP function is necessary for neuronal development, we quantified motor axon pathfinding defects in *Mmp1* and *Mmp2* single mutant embryos as well as *Mmp1 Mmp2* double mutants. In contrast to the hyperfasciculation phenotypes observed with MMP misexpression, MMP homozygous LOF mutants exhibit reduced fasciculation of the ISNb nerve (Table 2; Fig. 4). For *Mmp1*, we scored embryos homozygous mutant for a null allele, $Mmp1^{Q112*}$, as well as embryos heterozygous for $Mmp1^{Q112*}$ and $Mmp1^{2}$, a deletion removing almost all coding sequence (Page-McCaw et al., 2003). In embryos carrying either allelic combination of *Mmp1*, we found similar, if relatively mild, ISNb phenotypes. In affected hemisegments, ISNb pathfinding was roughly wild type, though the nerve was less tightly bundled and had a frayed appearance (compare Fig. 4A and B). Whereas 50% of $Mmp1^{Q112*}/Mmp1^{Q112*}$ hemisegments displayed a loosely fasciculated ISNb morphology, the penetrance fell to 28% for $Mmp1^{Q112*}/Mmp1^{2}$ embryos (Table 2), suggesting that a second-site mutation in the $Mmp1^{Q112*}$ line contributes to the observed ISNb phenotype.

For *Mmp2*, we analyzed embryos homozygous for the null allele, $Mmp2^{W307*}$, and embryos heterozygous for $Mmp2^{W307*}$ and $Mmp2^{Df(2R)Uba1\text{-}Mmp2}$ ($Mmp2^{Df}$), a deletion removing the first three coding exons of *Mmp2* (Page-McCaw et al., 2003). Embryos of both of these genotypes exhibited marked defects in ISNb fasciculation. The *Mmp2* LOF phenotypes included not only the loosely bundled morphology observed in *Mmp1* homozygotes, but also exuberant branching of the ISNb – with ectopic axonal projections splintering off inappropriately and extending improperly within the ventral longitudinal muscle field (compare Fig. 4A and C). Quantifying these phenotypes, we find that 85% of hemisegments from $Mmp2^{W307*}$ homozygotes and 74% of $Mmp2^{W307*}/Mmp2^{Df}$ hemisegments displayed either a frayed appearance or excessive projections (n=187 and 238; Table 2). The ISNb phenotypes apparent in both *Mmp1* and *Mmp2* homozygotes suggest that both MMPs contribute to proper bundling of the ISNb motor nerve branch, with *Mmp2* playing the major role.

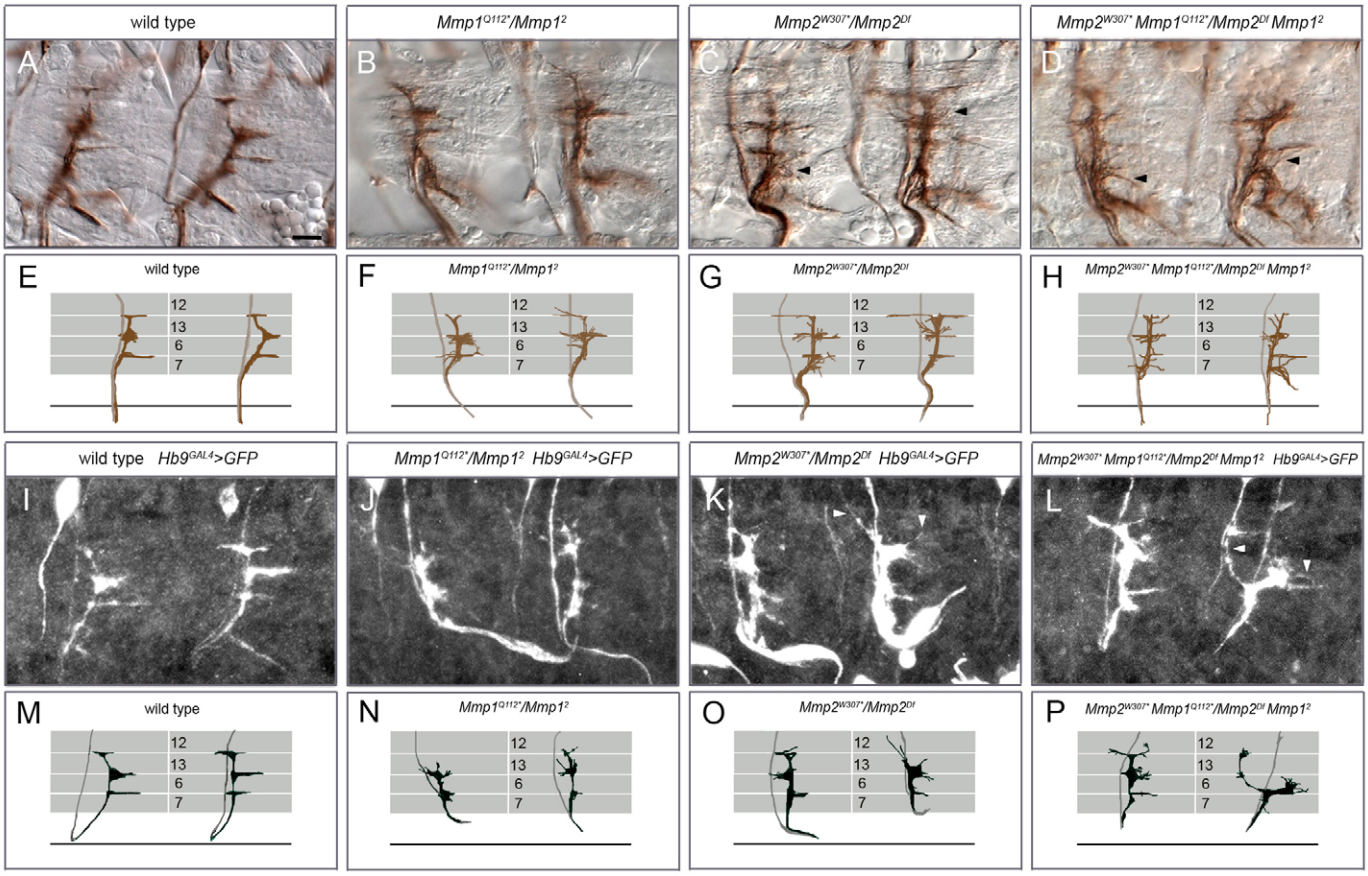

Fig. 4. MMP LOF mutants display inappropriate ISNb defasciculation. In each micrograph, two abdominal hemisegments of stage 17 dissected embryos stained with α-FasII (**A-D**) or α-GFP (**I-L**) to label the motor projections, are shown with anterior left and dorsal up. Below each image are schematics of the observed phenotypes with motor axons in brown (**E-H**) or black (**M-P**) and muscles represented by gray boxes. In addition to carrying mutations in the indicated MMP genes, embryos in I-L are heterozygous for both $Hb9^{Gal4}$ and *UAS-mCD8GFP* to visualize Hb9-positive axons with α-GFP. (A,E,I,M) Wild-type embryos have tightly bundled axonal projections. (B,F,J,N) $Mmp1^{Q112*}/Mmp1^{2}$ mutant embryos exhibit moderate ISNb defasciculation. (C,G,K,O) ISNb-projecting axons in $Mmp2^{W307*}/Mmp2^{Df}$ embryos are loosely bundled and frequently project aberrantly within the VLM field (arrowheads). (D,H,L,P) $Mmp2^{W307*}$ $Mmp1^{Q112*}/Mmp2^{Df}$ $Mmp1^{2}$ double mutants are indistinguishable from *Mmp2* single mutants with frequent ectopic projections (arrowheads). Scale bar: 15 μm.

Table 2. *Mmp1* and *Mmp2* loss of function mutant phenotypes

Genotype	Total aberrant ISNb† % (*n*)	Hyperfasciculation ISNb %	Hypofasciculation ISNb %	Total aberrant SNa % (*n*)	Hyperfasciculation SNa %	Hypofasciculation SNa %
Wild type	13 (140)	7	6	12 (138)	5	7
$Mmp1^{Q112*}/Mmp1^{Q112*}$	70 (175)	1	50	48 (132)	2	46
$Mmp1^{Q112*}/Mmp1^{2}$	74 (160)	1	28	39 (143)	3	36
$Mmp2^{W307*}/Mmp2^{W307*}$	90 (187)	1	85	45 (183)	3	42
$Mmp2^{W307*}/Mmp2^{Df}$	77 (238)	3	74	50 (248)	6	44
$Mmp2^{W307*}$ $Mmp1^{Q112*}$/ $Mmp2^{W307*}$ $Mmp1^{Q112*}$	86 (196)	0	79	61 (180)	3	58
$Mmp2^{W307*}$ $Mmp1^{Q112*}$/ $Mmp2^{Df}$ $Mmp1^{2}$	86 (175)	0	75	60 (186)	3	57

n, The number of hemisegments scored for each genotype.
†Includes hyperfasciculated, hypofasciculated and loss/reduction of the synapse in the 6/7 muscle cleft, which could be attributed to either hypo- or hyperfasciculation.

Analyses of MMP double mutants have provided evidence for redundancy between MMPs in vertebrates (Oh et al., 2004; Stickens et al., 2004). To determine if the incomplete penetrance observed in *Mmp1* and *Mmp2* single mutants might be explained by genetic redundancy between *Drosophila* MMPs, we quantified motor axon pathfinding defects in *Mmp1 Mmp2* double mutant embryos. We scored ISNb pathfinding in two different allelic combinations of *Mmp1 Mmp2* double mutants – $Mmp2^{W307*}$ $Mmp1^{Q112*}$ homozygotes and $Mmp2^{W307*}$ $Mmp1^{Q112*}/Mmp2^{Df}$ $Mmp1^{2}$. The guidance defects in the double mutants mirrored the phenotypes observed in *Mmp2* single mutants both qualitatively and quantitatively (Fig. 4D; Table 2). We observed both loosely associated ISNb axons and ISNb axons separating prematurely and ectopically from the main nerve branch. The frequency of the hypofasciculation phenotypes is roughly 75% in both double mutant allelic combinations. This penetrance is nearly identical to that observed for *Mmp2* single mutants, arguing that *Mmp1* activity does not substantially compensate for the loss of *Mmp2* function in promoting ISNb fasciculation.

To assess the LOF phenotypes in a second independent manner, we used $Hb9^{GAL4}$ to drive expression of membrane-bound GFP in MMP mutant embryos, thereby limiting visualization to axonal projections of ventrally and laterally projecting Hb9-positive motoneurons (Fig. 4I-P) (Broihier and Skeath, 2002). By focusing on the projections of Hb9-expressing neurons, we can exclude the possibility that the ectopic ISNb projections observed in MMP mutants are the result of misrouting of motor axons that normally extend in different pathways, such as Eve-positive dorsally projecting motor axons (Landgraf et al., 1999). $Hb9^{Gal4}$>*GFP Mmp1* single mutant embryos stained with anti-GFP displayed comparable fraying of the ISNb to those stained with FasII antibody (compare Fig. 4B and J). Similarly, $Hb9^{Gal4}$>*GFP Mmp2* single mutants and $Hb9^{Gal4}$>*GFP Mmp1 Mmp2* double mutant embryos continued to exhibit loosely bundled axons and ectopic branching of the ISNb when stained with anti-GFP (Fig. 4C,D,K,L). As ectopic ISNb projections are still frequently observed in these embryos, they likely correspond to misguided ISNb axons rather than motor axons misrouted from other pathways. These data support our quantitative FasII analysis and indicate that MMP activity is necessary for ISNb fasciculation.

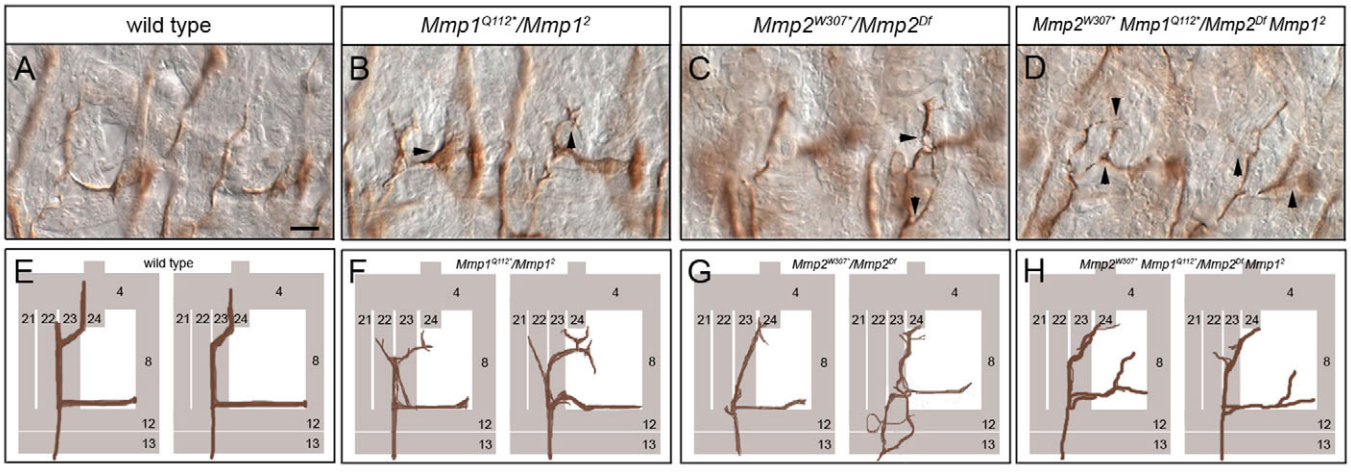

Fig. 5. MMP LOF mutants exhibit excessive SNa defasciculation. In each micrograph, two abdominal hemisegments of stage 17 dissected embryos stained with α-FasII to label the motor projections, are shown with anterior left and dorsal up. Below each image are schematics of the observed phenotypes with motor axons in brown and muscles represented by gray boxes. (**A**,**E**) In wild type, the two branches of the SNa stay tightly bundled after dividing into dorsal and posterior branches and go on to correctly innervate their lateral muscle targets. (**B**,**F**) In $Mmp1^{Q112*}/Mmp1^{2}$ embryos, axons within the dorsal and posterior SNa branches project ectopically (arrowheads). (**C**,**G**) $Mmp2^{W307*}/Mmp2^{Df}$ mutants display aberrant SNa defasciculation (arrowheads) phenotypes similar to those observed in *Mmp1* mutants. (**D**,**H**) SNa-projecting axons in $Mmp2^{W307*}$ $Mmp1^{Q112*}/Mmp2^{Df}$ $Mmp1^{2}$ double mutant embryos branch aberrantly and are less tightly bundled (arrowheads). The penetrance of SNa defasciculation observed in MMP double mutants is increased relative to either MMP single mutant. Scale bar: 15 μm.

To determine if MMP LOF phenotypes are limited to the ISNb branch, we quantified SNa morphology in single and double mutant MMP embryos. Similar to the phenotypes observed for ISNb, we find evidence of decreased SNa fasciculation in MMP mutant embryos. Embryos of all six single and double mutant allelic combinations displayed SNa phenotypes consistent with decreased axonal fasciculation (Table 2; Fig. 5). In most cases, axons branched prematurely or inappropriately from either the dorsal or posterior SNa secondary branches (arrowheads in Fig. 5B,C,D). Whereas *Mmp2* is primarily responsible for promoting ISNb fasciculation, we do not observe a statistically significant difference in the frequency of SNa defasciculation in *Mmp1* (36%) compared to *Mmp2* (44%) single mutants (P=0.1). These data indicate that *Mmp1* plays a relatively more significant role in SNa pathfinding than in ISNb pathfinding. Consistent with an increased genetic requirement for *Mmp1* activity in SNa fasciculation, mutant analysis indicates that *Mmp1* activity alone can promote substantial SNa fasciculation. In double mutant embryos, the penetrance of SNa defasciculation is significantly increased relative to that of either single mutant (Table 2). Specifically, 57% of double mutant hemisegments displayed ectopic SNa branches, relative to 36% for *Mmp1* mutants and 44% for *Mmp2* (P<0.05 for both). These data indicate that in contrast to ISNb, *Mmp1* and *Mmp2* serve partially redundant functions in SNa fasciculation. Together, our analyses indicate that MMP activity promotes motor axon fasciculation of multiple motor nerves in the embryo. Whereas *Mmp2* contributes significantly to fasciculation of both ISNb and SNa, we find that the role of *Mmp1* in pathfinding is largely specific to SNa.

Although our data suggest that MMPs are directly involved in pathfinding, in vertebrates MMPs have been shown to regulate processes as diverse as cell proliferation, survival, and differentiation (Page-McCaw et al., 2007). To address the possibility that MMPs might indirectly influence axon pathfinding by affecting earlier aspects of neurogenesis, we analyzed neuronal fate in MMP LOF and GOF mutants using a battery of molecular markers for distinct neuronal populations including anti-Eve, anti-Hb9, and anti-Nkx6 (Broihier et al., 2004; Broihier and Skeath, 2002). We do not detect any aberrations in neuronal fate specification in any MMP mutant background (C.M.M. and H.T.B., unpublished). The finding that MMPs do not appear to play a role in neural development prior to axon outgrowth is consistent with our expression analysis (see above) indicating that the MMP expression in the CNS initiates at stage 14 in post-mitotic neurons and glia.

Inhibition of MMP catalytic activity disrupts motor axon guidance

Our studies indicate that the level of MMP expression is a critical determinant of the degree of motor axon bundling. To test whether MMP catalytic activity regulates axon pathfinding, we specifically interfered with MMP catalytic activity by several different means. We first used a *UAS-Timp* construct to misexpress Timp (Tissue inhibitor of metalloproteinases) in embryonic neurons and glia via *elavGAL4* and *repoGAL4*, respectively. TIMPs are secreted protein inhibitors that interfere with MMP catalytic activity by binding to the active site of the enzyme (Gomis-Ruth et al., 1997). The *Drosophila* genome contains a single *Timp* gene that inhibits both *Mmp1* and *Mmp2* function in vivo (Page-McCaw et al., 2003). We

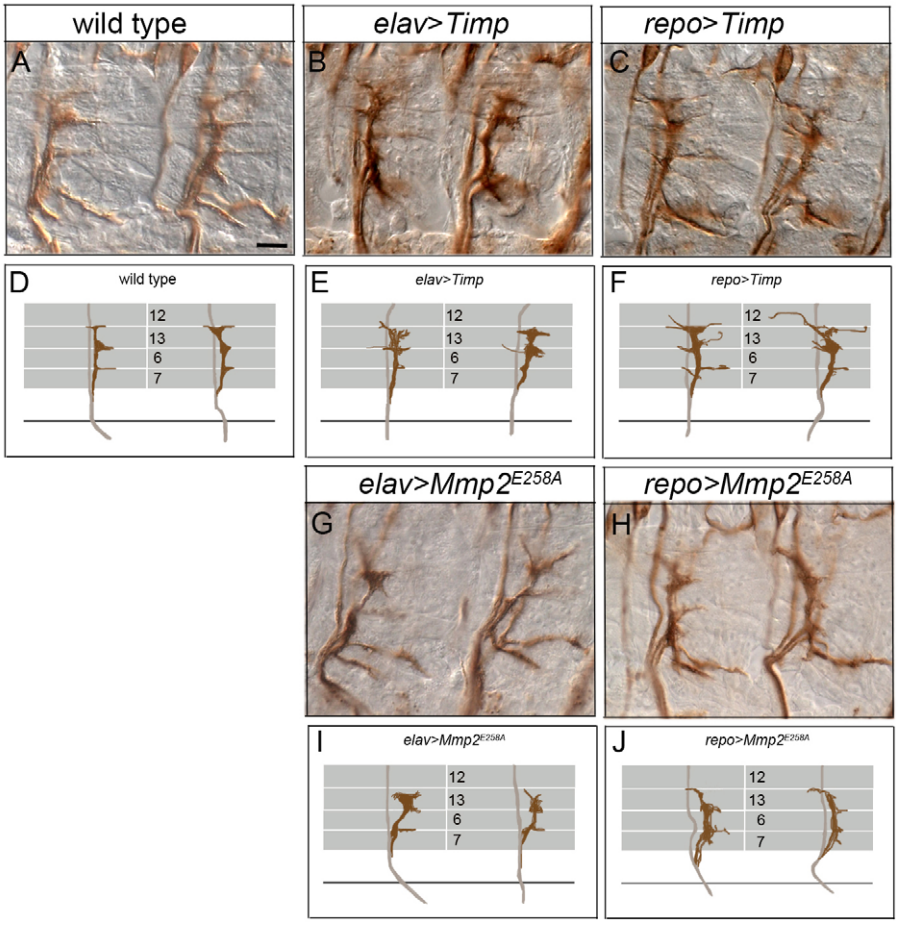

Fig. 6. MMP catalytic activity is required for motor axon pathfinding. In each micrograph, two abdominal hemisegments of Stage 17 dissected embryos stained with α-FasII to label the motor projections are shown with anterior left and dorsal up. Below each image are schematics of the observed phenotypes with motor axons in brown and muscles represented by gray boxes. (**A**,**D**) In wild type, the ISNb exhibits a highly stereotyped morphology as its axons innervate their muscle targets. (**B**,**E**) In *elav>Timp* embryos, ISNb axons appear loosely bundled. (**C**,**F**) In *repo>Timp* embryos, ISNb axons are loosely bundled and project ectopically. (**G**,**I**) *elav>Mmp2*^{E258A} embryos exhibit aberrant ISNb projections with axons failing to innervate their appropriate targets. (**H**,**J**) In *repo>Mmp2*^{E258A} embryos, ISNb axons are loosely bundled and often branch ectopically. Scale bar: 15 μm.

find that ISNb morphology is aberrant in *Timp* misexpression embryos (Table 1; Fig. 6B,C,E,F). Whereas ISNb axons are tightly bundled in wild type, they appeared disorganized with *Timp* misexpression. Individual axons were often apparent, suggesting the nerves are more loosely associated than in wild type. Additionally, axons separated inappropriately from the ISNb and extended over the VLM field, similar to the phenotype observed in *Mmp2* single and *Mmp1 Mmp2* double mutant embryos. To test the extent of the *Timp* misexpression phenotypes, we assayed SNa motor axon guidance. We find that SNa pathfinding is sensitive to *Timp* expression levels as SNa morphology is aberrant with *Timp* misexpression. Most commonly, we observed ectopic branches extending from either the dorsal or posterior SNa branches (Table 1). Thus, *Timp* misexpression gives phenotypes roughly comparable to those observed in MMP LOF mutants in two distinct motor pathways, suggesting that MMP enzymatic activity is required for proper motor axon fasciculation.

Although TIMPs are best characterized as MMP inhibitors, *Drosophila Timp* has been shown to interfere with the activity of other metalloproteinases (Wei et al., 2003), raising the possibility that *Timp* misexpression inhibits metalloproteinases other than MMPs in embryonic neuronal development.

Additionally, vertebrate MMP-MT1 regulates cell migration independent of its catalytic domain (Cao et al., 2004), suggesting that *Drosophila* MMPs could have proteolysis-independent functions. Therefore, we evaluated whether the neuronal overexpression of catalytically inactive MMPs impaired axon pathfinding. Overexpression of a catalytically inactive form of *Mmp1*, $Mmp1^{E225A}$, in cell culture acts as a dominant negative (Zhang et al., 2006), presumably by competing with wild-type Mmp1 for substrate binding. To determine whether overexpression of catalytically inactive forms of *Mmp1* and *Mmp2* interfered with MMP function in vivo, we tested whether misexpression of $Mmp1^{E225A}$ and an *Mmp2* mutant predicted to be catalytically inactive, $Mmp2^{E258A}$, disrupted motor axon pathfinding. We found that misexpression of either $Mmp1^{E225A}$ or $Mmp2^{E258A}$ had comparable effects on ISNb morphology to that of *Timp* misexpression (Table 1; Fig. 6G,H,I,J). Namely, the ISNb in these embryos exhibited defasciculation with loose bundling and ectopic branches. Interestingly, for $Mmp2^{E258A}$, we found that glial misexpression results in a significantly higher frequency of ISNb defects than does neural misexpression (50% vs 37%, respectively; $P<0.5$). This increased penetrance may be explained by the fact that Mmp2 is thought to be both membrane-tethered and normally expressed in glia, raising the possibility that a glial-derived catalytically inactive form of Mmp2 is better positioned to compete with the endogenous enzyme. It is also noteworthy that the defasciculation phenotypes observed with $Mmp1^{E225A}$ are stronger than those observed in *Mmp1* single LOF mutants (Tables 1 and 2), raising the possibility that the MMPs have overlapping substrate specificities (see Discussion). Together, the analyses of MMP LOF mutants and the MMP enzymatic inhibitor studies demonstrate that MMP catalytic activity is necessary for motor axon fasciculation.

MMPs promote FasII-dependent motor axon adhesion and antagonize *Sema-1a* signaling

Motor axon pathfinding is regulated by the interplay of factors that promote axon bundling such as cell adhesion molecules, and factors that antagonize motor axon adhesion to enable motor axon defasciculation at defined choice points. In the *Drosophila* embryo, motor axon defasciculation is controlled in part by the action of the *Sema-1a-plexA* signaling pathway (Winberg et al., 1998b; Yu et al., 1998). A number of classic genetic interaction studies have demonstrated that the relative strength of attractive and repulsive cues is critical for axon guidance. For example, the ISNb phenotype of *Sema-1a* mutant embryos is dominantly suppressed by mutations in the cell adhesion molecule *FasII* (Yu et al., 2000). The *FasII* suppression of *Sema-1a* LOF mutants provides strong support for the hypothesis that the balance of forces promoting and inhibiting motor axon adhesion is precisely regulated to ensure that defasciculation is tightly controlled. Our phenotypic analysis suggests that MMP activity promotes motor axon fasciculation and thus acts in concert with *Fas2* and in opposition to the repulsive signaling mediated by *Sema-1a* and *plexA*. This model predicts that the excessive axon defasciculation displayed by MMP mutants would be suppressed by otherwise elevating interaxonal adhesion. We first tested this hypothesis by asking if *Timp* misexpression could counteract the motor axon hyperfasciculation observed with pan-neuronal overexpression of *Fas2*. *elav>Fas2* overexpression embryos display a high degree of ISNb hyperfasciculation, with many hemisegments displaying either a 'bypass' or 'detour' phenotype (Lin and Goodman, 1994). The detour phenotype resembles the bypass phenotype in that ISNb motor axons fail to exit the ISN at their first choice point. In detour hemisegments, however, some ISNb axons go on to separate from the ISN at more dorsal positions and enter the VLM field (arrowhead in Fig. 7B). We find that the extent of ISNb hyperfasciculation induced by *Fas2* overexpression is significantly suppressed by co-overexpression of

Table 3. *MMP/Timp* genetic interactions

Genotype	Total aberrant ISNb† % (*n*)	Hyperfasciculation ISNb %			Hypofasciculation ISNb %	Total aberrant SNa % (*n*)	Hyperfasciculation SNa %	Hypofasciculation SNa %
		Fusion bypass	Detour	Stall				
Wild type	13 (140)	0	0	7	6	12 (138)	5	7
elav>Fas2	84 (160)	27	28	26	0	NS	NS	NS
elav>Fas2, Timp	87 (247)	11	15	42	0	NS	NS	NS
$Mmp1^{Q112*}/Mmp1^{2}$	74 (160)	0	0	1	28	39 (143)	3	36
$Sema\text{-}1a^{P1}$ $Mmp1^{Q112*}/+$ $Mmp1^{2}$	72 (118)	1	0	8	25	35 (113)	16	19
$Mmp2^{W307*}/Mmp2^{Df}$	77 (238)	0	0	3	74	50 (248)	6	44
$Sema\text{-}1a^{P1}$ $Mmp2^{W307*}/+$ $Mmp2^{Df}$	54 (178)	0	0	5	39	39 (169)	8	32

n, The number of hemisegments scored for each genotype.
NS, not scored.
†Includes hyperfasciculated, hypofasciculated and loss/reduction of the synapse in the 6/7 muscle cleft, which could be attributed to either hypo- or hyperfasciculation.

Timp (Table 3; compare Fig. 7B and C). The frequency of bypass phenotypes decreases from 27% in *elav>Fas2* embryos to 11% in *elav>Fas2, Timp* embryos. Similarly, the frequency of detour phenotypes is reduced from 28% in *elav>Fas2* embryos to 15% in *elav>Fas2, Timp* embryos ($P<0.05$ for both phenotypic classes). The *Timp*-mediated suppression of ISNb hyperfasciculation observed with *Fas2* overexpression indicates that MMP activity normally promotes *Fas2*-dependent motor axon adhesion.

To provide additional evidence that MMPs are required for motor axon fasciculation, we asked whether they normally act in opposition to the *Sema-1a-plexA* pathway by testing whether MMP LOF mutant phenotypes are dominantly suppressed by a null allele of *Sema-1a*. In fact, we find that the penetrance of ISNb defasciculation in *Mmp2* mutants is significantly reduced in a *Sema-1a* heterozygous background (Table 3; Fig. 7G-L). In particular, the frequency of loose bundling/ectopic branches for ISNb is decreased roughly twofold: from 74% in $Mmp2^{W307*}/Mmp2^{Df}$ heterozygotes to 39% in $Sema\text{-}1a^{P1}$ $Mmp2^{W307*}/+$ $Mmp2^{Df}$ embryos. The *Sema-1a* suppression of *Mmp2* LOF mutations demonstrates that *Mmp2* activity normally counteracts *Sema-1a*-mediated repulsive signaling to regulate defasciculation of the ISNb motor projection. By contrast, the mild ISNb defects observed in *Mmp1* single mutants are not dominantly suppressed by *Sema-1a* (Table 3), in agreement with our phenotypic analysis indicating that *Mmp1* does not contribute significantly to ISNb fasciculation. Since the aberrant motor axon defasciculation observed in MMP mutants is not limited to the ISNb, we wanted to determine whether the pathfinding defects apparent in the SNa pathway were also suppressed by reducing *Sema-1a* dosage. Therefore, we compared the penetrance of SNa defects in *Mmp1* and *Mmp2* single mutants to those observed in MMP mutants in a heterozygous *Sema-1a* background. The excessive defasciculation apparent in SNa in *Mmp1* and *Mmp2* mutants is also suppressed by reducing *Sema-1a* dosage (Table 3), though the suppression is not as strong as was observed for *Mmp2* mutants in ISNb. The modest suppression observed is consistent with published data demonstrating that the relatively large number of adhesion molecules promoting fasciculation of SNa decreases the strength of genetic interactions between any two factors (Yu et al., 2000). Combined with the strong dominant suppression observed for ISNb, these data demonstrate a critical and widespread role for MMPs in achieving the required balance between attractive and repulsive factors underlying proper axon pathfinding.

DISCUSSION

This work demonstrates that the level of MMP catalytic activity dictates the degree of motor axon fasciculation in the *Drosophila* embryo. MMP misexpression is sufficient to inhibit separation of motor axons during outgrowth, but both of the primary embryonic motor nerve branches display striking defasciculation in MMP LOF mutants. The opposing axonal phenotypes observed in MMP LOF and GOF embryos indicates that the level of MMP activity is critical for pathfinding and further suggests that the relevant MMP substrate(s) plays an instructive role in motor axon guidance. In support of the hypothesis that MMPs influence axon outgrowth by modulating the activity of established guidance cues, we show that *Mmp2* LOF mutants are dominantly suppressed by a null mutation in *Sema-1a*, arguing that MMP function is tightly coupled to guidance decisions. Here we discuss possible substrates for *Mmp2*

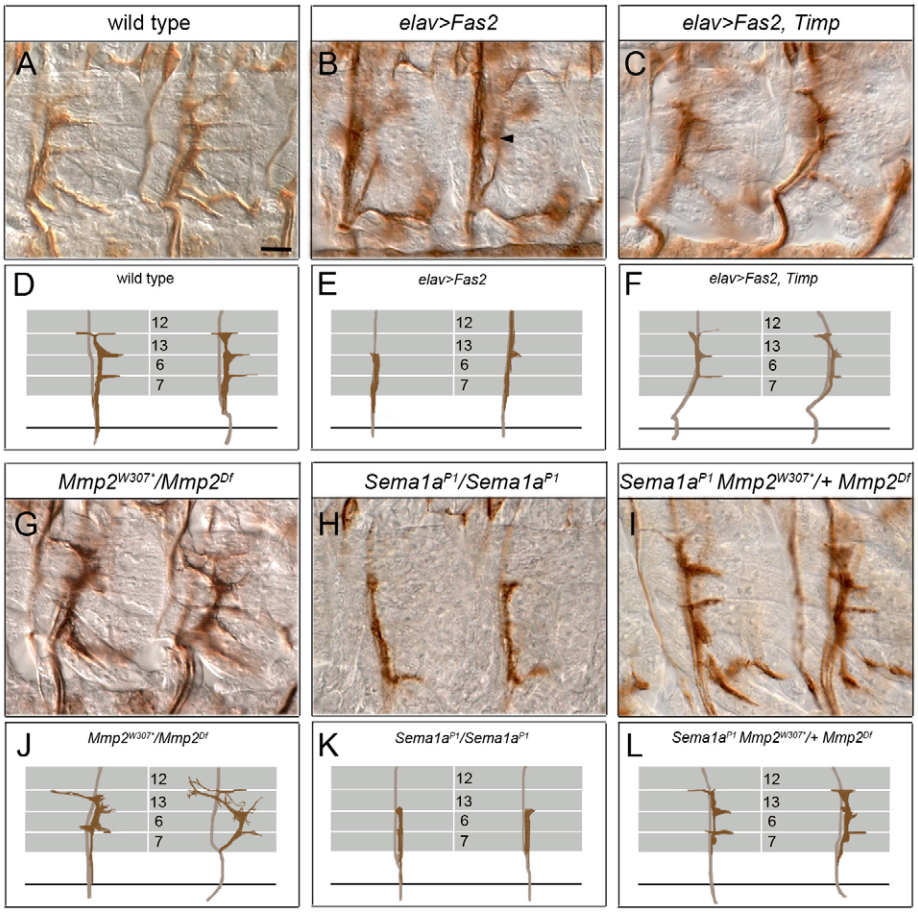

Fig. 7. The inappropriate defasciculation observed in mutants with reduced MMP activity is suppressed by increasing interaxonal adhesion. In each micrograph, two abdominal hemisegments of stage 17 dissected embryos stained with α-FasII to label the motor projections are shown with anterior left and dorsal up. Below each image are schematics of the observed phenotypes with motor axons in brown and muscles represented by gray boxes. (**A**,**D**) Wild-type embryo exhibiting normal ISNb morphology. (**B**,**E**) *elav>Fas2* mutant embryos have increased motor axon adhesion. (**C**,**F**) *elav>Fas2, Timp* embryos exhibit phenotypes consistent with weakened interaxonal adhesion relative to *elav>Fas2* embryos. (**G**,**J**) $Mmp2^{W307*}/Mmp2^{Df}$ mutant embryos have loosely bundled ISNb axons and ectopic branching. (**H**,**K**) The ISNb of $Sema\text{-}1a^{P1}/Sema\text{-}1a^{P1}$ mutant embryos exhibits hyperfasciculation and does not properly innervate its muscle targets. (**I**,**L**) In $Sema\text{-}1a^{P1}$ $Mmp2^{W307*}/+$ $Mmp2^{Df}$ mutant embryos, ISNb morphology resembles that of wild-type embryos. Note that these embryos have more tightly bundled nerves than do the *Mmp2* homozygous mutants shown in G. Scale bar: 15 μm.

in motor axon pathfinding and put our findings in the context of proposed neural functions for metalloproteinases in vertebrates and invertebrates.

Mmp1 and *Mmp2* are required for *Drosophila* embryonic CNS development

Both fly MMPs were previously shown to be expressed in the embryonic CNS (Llano et al., 2002; Llano et al., 2000; Page-McCaw et al., 2003), suggesting that they regulate aspects of neuronal development. However, the finding that both MMP single mutants and the *Mmp1 Mmp2* double mutant survived embryogenesis called into question the extent of any possible roles for the MMPs in embryogenesis (Page-McCaw et al., 2003). In this work we present genetic evidence that MMP catalytic activity is essential for motor axon fasciculation. Whereas *Mmp1* mutants display subtle fasciculation errors, we find that motor axons in *Mmp2* mutants are markedly defasciculated, with many embryonic nerves appearing frayed and poorly organized. Consistent with this phenotypic analysis, the CNS expression profile of *Mmp2* is considerably broader than that of *Mmp1*: *Mmp2* is expressed in midline glia, in clusters of interneurons and in peripheral/exit glia but CNS expression of *Mmp1* is limited to the midline. The prominent expression of *Mmp1* and *Mmp2* at the CNS midline prompted us to examine whether either MMP might be required for proper guidance there. However, we do not find any alterations in the behavior of axons at the midline in either MMP LOF or GOF mutant backgrounds or any genetic interactions between *Mmp2* and *Slit* or *Mmp1* and *Robo* (C.M.M. and H.T.B., unpublished). These data indicate that MMPs do not contribute significantly to embryonic midline guidance in the fly.

Although the *Mmp1* and *Mmp2* LOF phenotypes are distinct, several pieces of evidence suggest that they have overlapping substrate specificities and can cleave the same guidance cue(s). First, misexpression of either *Mmp1* or *Mmp2* yields qualitatively indistinguishable guidance phenotypes with many motor axons remaining inappropriately bundled together. Second, misexpression of an *Mmp1* dominant-negative transgene gives phenotypes nearly identical to those observed with a dominant negative *Mmp2*. Furthermore, the phenotypes observed with these constructs are stronger and more penetrant than the phenotypes of *Mmp1* LOF mutants (Tables 1 and 2), suggesting that the *Mmp1* dominant-negative transgene affects motor axon pathfinding by interfering with *Mmp2* function by binding to the relevant *Mmp2* substrate(s). Lastly, if *Mmp1* and *Mmp2* cleave the same substrate(s), they might be expected to be genetically redundant, as removal of one would be compensated for by the presence of the other. In fact, we have shown that *Mmp1* and *Mmp2* play partially redundant roles in SNa pathfinding, as the double mutant phenotype is significantly stronger than the phenotype observed in either single mutant. These results are in agreement with analyses of enzymatic activity of vertebrate MMPs that suggest that there is overlap between the substrates cleaved by individual MMPs (Page-McCaw et al., 2007).

Mmp2 contains a predicted GPI anchor and is membrane associated in *Drosophila* tissue culture cells (Llano et al., 2002). Thus, the expression pattern of *Mmp2* in the embryo would be expected to reflect the locations of Mmp2-dependent proteolysis. We find *Mmp2* RNA to be expressed in restricted populations of interneurons and peripheral glia, but not in motoneurons (Fig. 2). Peripheral glia originate at the lateral edge of the CNS and migrate into the periphery along elongating motor axons. By the end of embryogenesis, they extend cytoplasmic processes and wrap axon bundles in a manner similar to vertebrate non-myelinating Schwann cells (Jacobs and Goodman, 1989; Sepp et al., 2000; Sepp et al., 2001). We propose that peripheral glial-derived *Mmp2* modulates the activity of factors required for pathfinding. This model implies that peripheral glia play a significant role in regulating motor axon fasciculation. This finding contrasts slightly with the results of Sepp et al. (Sepp et al., 2001) who found more subtle errors in the motor axon projection pattern when peripheral glia were genetically ablated. One possible explanation for the weaker phenotypes in the peripheral glia-ablated embryos relative to *Mmp2* LOF mutants is that peripheral glia express several factors that influence axon pathfinding in opposing directions – for example, proteins that both inhibit and stimulate fasciculation. In this way, peripheral glia would somewhat resemble midline glia which express both an axonal attractant (Netrin) and repellent (Slit) (Dickson, 2002). Therefore, ablation of the entire cellular population would be expected to yield different phenotypes than mutating individual molecules. Another possibility is that although *Mmp2* is likely to act locally, its substrate might be secreted and could regulate motor axon guidance at a distance. In this case, *Mmp2* need not be expressed at the site of fasciculation decisions, and either midline or interneuron-derived *Mmp2* might provide the relevant proteolytic activity.

What guidance cues could be MMP targets in *Drosophila* motor axon pathfinding?

In principle, since MMP cleavage might either activate or inhibit the function of a molecule required for axon guidance, the motor axon phenotypes observed in MMP mutants could be expected to be identical to or opposite that of the phenotypes displayed by substrate mutations. Based solely on phenotypic considerations, several guidance molecules could be considered candidate MMP substrates. For example, LOF mutations in a number of genes give hyperfasciculation and/or stalled motor axon phenotypes. These include *beaten path* (*beat*) and *sidestep* (*side*), two immunoglobulin superfamily proteins required for proper defasciculation of both ISNb and SNa (Fambrough and Goodman, 1996; Sink et al., 2001). There are also five CNS-expressed receptor protein tyrosine phosphatases (RPTPs) that have combinatorial roles in the regulation of motor axon pathfinding. A number of these RPTPs, in particular LAR, are involved in ISNb defasciculation decisions (Desai et al., 1997; Schindelholz et al., 2001). Additionally, Plexin proteins and their receptors, the semaphorins, are critical regulators of motor axon fasciculation. Sema-Plex pathway activity promotes inter-axonal repulsion so that LOF mutations in Sema-Plex pathway components result in ISNb stall phenotypes (Ayoob et al., 2006; Terman et al., 2002; Winberg et al., 1998a; Yu et al., 1998). Importantly, it has also been shown that for axons to remain tightly bundled during normal axon outgrowth, Sema-Plex signaling must be actively antagonized, as LOF mutations in two downstream inhibitors, *nervy* and *Protein kinase A*, give aberrant defasciculation phenotypes similar to that observed in MMP mutations (Terman and Kolodkin, 2004). Hence, levels of *Sema-plex* activity must be tightly controlled to ensure that defasciculation occurs properly at guidance choice points. And similar to what we describe here for MMPs, reciprocal GOF and LOF mutations in the pathway can result in opposing hyper- and hypo-fasciculation phenotypes.

The MMP family as a whole does not cleave a conserved amino acid sequence in their targets, meaning that *Drosophila* substrates must be determined empirically, not computationally. One identified *Mmp1* substrate, *Ninjurin A* (*NijA*), represented an appealing candidate in motor axon guidance as it is a signaling protein that regulates cell adhesion whose vertebrate homologs are upregulated in response to nerve injury (Zhang et al., 2006). However, we do not

detect any aberrations to motor axon pathfinding in either *NijA* LOF or GOF mutants (C.M.M. and H.T.B., unpublished), indicating that *NijA* is unlikely to be a relevant substrate in this context. Although few other *Drosophila* MMP substrates have been identified, the *Drosophila* homologs of several putative vertebrate MMP substrates make appealing candidates for MMP targets in embryonic CNS development. For instance, vertebrate membrane type MMP1 (MT1-MMP), has been shown to interact with the transmembrane heparan sulfate proteoglycan Syndecan 1 and trigger Syndecan 1 ectodomain shedding (Endo et al., 2003). Syndecan 1 processing stimulated cell migration on collagen, suggesting that this cleavage has functional consequences in vivo. Interestingly, Fox and Zinn (Fox and Zinn, 2005) identified *Drosophila* Syndecan (Sdc) as a ligand for the LAR RPTP. Accordingly, genetic interaction studies indicate that Sdc and LAR act in concert to regulate ISNb pathfinding. As it is currently unknown whether LAR binds membrane-bound or soluble Sdc, MMP activity could potentially regulate the LAR/Sdc interaction. In addition, MT1-MMP has also recently been shown to be required for ectodomain shedding of Semaphorin 4D in a model of tumor-induced angiogenesis – a processing event required for the induction of blood vessel growth in vivo (Basile et al., 2007). As discussed above, Semaphorin signaling plays a well-documented role in regulating motor axon behavior. Furthermore, since we have found that *Sema-1a* mutations display strong genetic interactions with *Mmp2* mutations in this system, it is conceivable that MMPs directly modulate Sema-Plex signaling activity.

Metalloproteinases serve constructive functions in the CNS

MMP expression levels are highly elevated in a number of neuronal pathologies and after nervous system injury. MMP upregulation in CNS disease states raises the issue of whether MMP induction has an overall positive or negative effect on disease outcome. There is substantial evidence that the net effect of high MMP expression in some diseases is detrimental (Yong, 2005; Yong et al., 2001). For example, treatment with broad-spectrum metalloproteinase inhibitors is able to alleviate or prevent experimental autoimmune encephalomyelitis (EAE), a mouse multiple sclerosis model (Chandler et al., 1997; Yong et al., 1998). There is also, however, growing recognition of beneficial functions for MMPs following CNS injury. The diverse functions for MMPs in disease states have become increasingly apparent as investigators have moved beyond the use of general metalloproteinase inhibitors to the study of particular MMPs. For example, increased expression of individual MMPs has been shown to correlate with periods of regeneration and repair following nervous system injury (Ahmed et al., 2005; Demestre et al., 2004; Shubayev and Myers, 2004). The functional significance of elevated MMP expression on regenerating axons has not been established, though in some regeneration models treatment with active MMPs promotes axon outgrowth (Heine et al., 2004; Siebert et al., 2001). In regeneration, it is thought that MMPs influence axon growth by degrading chondroitin sulphate proteoglycans (CSPGs), which normally inhibit regrowth beyond the glial scar.

In the context of neuronal development, there is substantial support for the idea that metalloproteinases, and in particular the ADAM subfamily, regulate axon outgrowth and pathfinding (McFarlane, 2003). Early work in the field suggested that metalloproteinases play a largely permissive role in axon outgrowth – by degrading the ECM in order to clear a path for extending axons (Muir, 1994; Nordstrom et al., 1995; Zuo et al., 1998). In support of a role for MMPs in outgrowth, it has been shown that a number of MMPs are expressed on the growth cones of vertebrate neurites extending in vitro (Chambaut-Guerin et al., 2000; Hayashita-Kinoh et al., 2001; Nordstrom et al., 1995; Zuo et al., 1998). More recent work has demonstrated that in vitro, metalloproteinases are capable of modulating the interactions between guidance cues and their receptors (Galko and Tessier-Lavigne, 2000; Hattori et al., 2000). For example, the interaction between ephrin A2 and Eph receptor is terminated by ephrin A2 cleavage via ADAM10 (also known as Kuzbanian-like – FlyBase) and/or Kuz. Functionally, this cleavage allows growth cone withdrawal of hippocampal neurons in culture, as a cleavage-inhibiting mutation delays axon retraction (Hattori et al., 2000). Metalloproteinases have also been implicated in DCC (deleted in colorectal carcinoma) receptor activity as broad-spectrum metalloproteinase inhibitors inhibit ectodomain shedding of DCC and potentiate netrin-mediated axon outgrowth (Galko and Tessier-Lavigne, 2000). In vivo support for the role of ADAM proteases in axon outgrowth and pathfinding comes from work in *Drosophila* (Fambrough et al., 1996; Schimmelpfeng et al., 2001). *kuz* mutant embryos display ectopic axon crossing at the midline suggesting that *kuz* is required for repulsive signaling mediated by Slit-Roundabout (Robo). Supporting this idea, *kuz* and *slit* mutations genetically interact, and Kuz appears to be required for the clearance of the Robo receptor from commissural axons (Schimmelpfeng et al., 2001).

Although a number of vertebrate MMPs display neuronal expression patterns in the embryo (Gonthier et al., 2007; Hayashita-Kinoh et al., 2001; Jaworski, 2000; Sekine-Aizawa et al., 2001), until relatively recently there was little direct evidence supporting a role for this metalloproteinase subclass in axon pathfinding. Studies of retinal ganglion cell (RGC) pathfinding in frogs argue that MMP activity is required for axon guidance at several defined choice points. Hehr et al. (Hehr et al., 2005) used an MMP-specific inhibitor to demonstrate that MMPs are required for RGC guidance decisions both at the optic chiasm and tectum. This work suggested that MMPs are normally required for axon guidance during vertebrate development, though the particular MMPs involved in RGC pathfinding remain to be identified. Exploiting the relative simplicity of the *Drosophila* model system, we have now established that individual MMPs play critical and distinct roles in well-defined axon pathfinding decisions during development. To extend this work to more complex vertebrate systems, it will be critical to analyze axon outgrowth and pathfinding in MMP single and compound mutant mice.

We are indebted to Aaron DiAntonio and Jim Skeath for their generous support and contributions to the misexpression screen that led to the identification of *Mmp1*. We thank Julia Serrano for generating the *Mmp2*^{E258A} construct and transgenic lines and Julie Simpson, Alex Kolodkin and Marc Freeman for fly stocks. We are also grateful to Jocelyn McDonald, Kate O'Connor-Giles, and members of the Broihier lab for critical comments on the manuscript. This work was supported by NIH RO1NS055245 and the Mt. Sinai Foundation to H.T.B.; by NIH training grant AG00271 to C.M.M.; and by NIH R01GM073883 to A.P.-M.

References

Ahmed, Z., Dent, R. G., Leadbeater, W. E., Smith, C., Berry, M. and Logan, A. (2005). Matrix metalloproteases: degradation of the inhibitory environment of the transected optic nerve and the scar by regenerating axons. *Mol. Cell. Neurosci.* **28**, 64-78.

Ayoob, J. C., Terman, J. R. and Kolodkin, A. L. (2006). *Drosophila* Plexin B is a Sema-2a receptor required for axon guidance. *Development* **133**, 2125-2135.

Basile, J. R., Holmbeck, K., Bugge, T. H. and Gutkind, J. S. (2007). MT1-MMP controls tumor-induced angiogenesis through the release of semaphorin 4D. *J. Biol. Chem.* **282**, 6899-6905.

Broihier, H. T. and Skeath, J. B. (2002). Drosophila homeodomain protein dHb9 directs neuronal fate via crossrepressive and cell-nonautonomous mechanisms. *Neuron* **35**, 39-50.
Broihier, H. T., Kuzin, A., Zhu, Y., Odenwald, W. and Skeath, J. B. (2004). *Drosophila* homeodomain protein Nkx6 coordinates motoneuron subtype identity and axonogenesis. *Development* **131**, 5233-5242.
Cao, J., Kozarekar, P., Pavlaki, M., Chiarelli, C., Bahou, W. F. and Zucker, S. (2004). Distinct roles for the catalytic and hemopexin domains of membrane type-1 matrix metalloproteinase in substrate degradation and cell migration. *J. Biol. Chem.* **279**, 14129-14139.
Chambaut-Guerin, A. M., Herigault, S., Rouet-Benzineb, P., Rouher, C. and Lafuma, C. (2000). Induction of matrix metalloproteinase MMP-9 (92-kDa gelatinase) by retinoic acid in human neuroblastoma SKNBE cells: relevance to neuronal differentiation. *J. Neurochem.* **74**, 508-517.
Chandler, S., Miller, K. M., Clements, J. M., Lury, J., Corkill, D., Anthony, D. C., Adams, S. E. and Gearing, A. J. (1997). Matrix metalloproteinases, tumor necrosis factor and multiple sclerosis: an overview. *J. Neuroimmunol.* **72**, 155-161.
Demestre, M., Wells, G. M., Miller, K. M., Smith, K. J., Hughes, R. A., Gearing, A. J. and Gregson, N. A. (2004). Characterisation of matrix metalloproteinases and the effects of a broad-spectrum inhibitor (BB-1101) in peripheral nerve regeneration. *Neuroscience* **124**, 767-779.
Desai, C. J., Krueger, N. X., Saito, H. and Zinn, K. (1997). Competition and cooperation among receptor tyrosine phosphatases control motoneuron growth cone guidance in *Drosophila*. *Development* **124**, 1941-1952.
DiAntonio, A., Haghighi, A. P., Portman, S. L., Lee, J. D., Amaranto, A. M. and Goodman, C. S. (2001). Ubiquitination-dependent mechanisms regulate synaptic growth and function. *Nature* **412**, 449-452.
Dickson, B. J. (2002). Molecular mechanisms of axon guidance. *Science* **298**, 1959-1964.
Endo, K., Takino, T., Miyamori, H., Kinsen, H., Yoshizaki, T., Furukawa, M. and Sato, H. (2003). Cleavage of syndecan-1 by membrane type matrix metalloproteinase-1 stimulates cell migration. *J. Biol. Chem.* **278**, 40764-40770.
Fambrough, D. and Goodman, C. S. (1996). The Drosophila beaten path gene encodes a novel secreted protein that regulates defasciculation at motor axon choice points. *Cell* **87**, 1049-1058.
Fambrough, D., Pan, D., Rubin, G. M. and Goodman, C. S. (1996). The cell surface metalloprotease/disintegrin Kuzbanian is required for axonal extension in Drosophila. *Proc. Natl. Acad. Sci. USA* **93**, 13233-13238.
Fox, A. N. and Zinn, K. (2005). The heparan sulfate proteoglycan syndecan is an in vivo ligand for the Drosophila LAR receptor tyrosine phosphatase. *Curr. Biol.* **15**, 1701-1711.
Galko, M. J. and Tessier-Lavigne, M. (2000). Function of an axonal chemoattractant modulated by metalloprotease activity. *Science* **289**, 1365-1367.
Gomis-Ruth, F. X., Maskos, K., Betz, M., Bergner, A., Huber, R., Suzuki, K., Yoshida, N., Nagase, H., Brew, K., Bourenkov, G. P. et al. (1997). Mechanism of inhibition of the human matrix metalloproteinase stromelysin-1 by TIMP-1. *Nature* **389**, 77-81.
Gonthier, B., Nasarre, C., Roth, L., Perraut, M., Thomasset, N., Roussel, G., Aunis, D. and Bagnard, D. (2007). Functional interaction between matrix metalloproteinase-3 and semaphorin-3c during cortical axonal growth and guidance. *Cereb. Cortex* **17**, 1712-1721.
Hattori, M., Osterfield, M. and Flanagan, J. G. (2000). Regulated cleavage of a contact-mediated axon repellent. *Science* **289**, 1360-1365.
Hayashita-Kinoh, H., Kinoh, H., Okada, A., Komori, K., Itoh, Y., Chiba, T., Kajita, M., Yana, I. and Seiki, M. (2001). Membrane-type 5 matrix metalloproteinase is expressed in differentiated neurons and regulates axonal growth. *Cell Growth Differ.* **12**, 573-580.
Hehr, C. L., Hocking, J. C. and McFarlane, S. (2005). Matrix metalloproteinases are required for retinal ganglion cell axon guidance at select decision points. *Development* **132**, 3371-3379.
Heine, W., Conant, K., Griffin, J. W. and Hoke, A. (2004). Transplanted neural stem cells promote axonal regeneration through chronically denervated peripheral nerves. *Exp. Neurol.* **189**, 231-240.
Jacobs, J. R. and Goodman, C. S. (1989). Embryonic development of axon pathways in the Drosophila CNS. I. A glial scaffold appears before the first growth cones. *J. Neurosci.* **9**, 2402-2411.
Jaworski, D. M. (2000). Developmental regulation of membrane type-5 matrix metalloproteinase (MT5-MMP) expression in the rat nervous system. *Brain Res.* **860**, 174-177.
Johnson, K. G., Ghose, A., Epstein, E., Lincecum, J., O'Connor, M. B. and Van Vactor, D. (2004). Axonal heparan sulfate proteoglycans regulate the distribution and efficiency of the repellent slit during midline axon guidance. *Curr. Biol.* **14**, 499-504.
Jones, B. W., Fetter, R. D., Tear, G. and Goodman, C. S. (1995). glial cells missing: a genetic switch that controls glial versus neuronal fate. *Cell* **82**, 1013-1023.
Klambt, C. and Goodman, C. S. (1991). The diversity and pattern of glia during axon pathway formation in the Drosophila embryo. *Glia* **4**, 205-213.
Landgraf, M., Bossing, T., Technau, G. M. and Bate, M. (1997). The origin, location, and projections of the embryonic abdominal motorneurons of Drosophila. *J. Neurosci.* **17**, 9642-9655.
Landgraf, M., Roy, S., Prokop, A., VijayRaghavan, K. and Bate, M. (1999). even-skipped determines the dorsal growth of motor axons in Drosophila. *Neuron* **22**, 43-52.
Llano, E., Pendas, A. M., Aza-Blanc, P., Kornberg, T. B. and Lopez-Otin, C. (2000). Dm1-MMP, a matrix metalloproteinase from Drosophila with a potential role in extracellular matrix remodeling during neural development. *J. Biol. Chem.* **275**, 35978-35985.
Llano, E., Adam, G., Pendas, A. M., Quesada, V., Sanchez, L. M., Santamaria, I., Noselli, S. and Lopez-Otin, C. (2002). Structural and enzymatic characterization of Drosophila Dm2-MMP, a membrane-bound matrix metalloproteinase with tissue-specific expression. *J. Biol. Chem.* **277**, 23321-23329.
McFarlane, S. (2003). Metalloproteases: carving out a role in axon guidance. *Neuron* **37**, 559-562.
Meyer, F. and Aberle, H. (2006). At the next stop sign turn right: the metalloprotease Tolloid-related 1 controls defasciculation of motor axons in *Drosophila*. *Development* **133**, 4035-4044.
Muir, D. (1994). Metalloproteinase-dependent neurite outgrowth within a synthetic extracellular matrix is induced by nerve growth factor. *Exp. Cell Res.* **210**, 243-252.
Noordermeer, J. N., Kopczynski, C. C., Fetter, R. D., Bland, K. S., Chen, W. Y. and Goodman, C. S. (1998). Wrapper, a novel member of the Ig superfamily, is expressed by midline glia and is required for them to ensheath commissural axons in Drosophila. *Neuron* **21**, 991-1001.
Nordstrom, L. A., Lochner, J., Yeung, W. and Ciment, G. (1995). The metalloproteinase stromelysin-1 (transin) mediates PC12 cell growth cone invasiveness through basal laminae. *Mol. Cell. Neurosci.* **6**, 56-68.
Oh, J., Takahashi, R., Adachi, E., Kondo, S., Kuratomi, S., Noma, A., Alexander, D. B., Motoda, H., Okada, A., Seiki, M. et al. (2004). Mutations in two matrix metalloproteinase genes, MMP-2 and MT1-MMP, are synthetic lethal in mice. *Oncogene* **23**, 5041-5048.
Page-McCaw, A., Serano, J., Sante, J. M. and Rubin, G. M. (2003). Drosophila matrix metalloproteinases are required for tissue remodeling, but not embryonic development. *Dev. Cell* **4**, 95-106.
Page-McCaw, A., Ewald, A. J. and Werb, Z. (2007). Matrix metalloproteinases and the regulation of tissue remodelling. *Nat. Rev. Mol. Cell Biol.* **8**, 221-233.
Parker, L., Ellis, J. E., Nguyen, M. Q. and Arora, K. (2006). The divergent TGF-beta ligand Dawdle utilizes an activin pathway to influence axon guidance in *Drosophila*. *Development* **133**, 4981-4991.
Rorth, P., Szabo, K., Bailey, A., Laverty, T., Rehm, J., Rubin, G. M., Weigmann, K., Milan, M., Benes, V., Ansorge, W. et al. (1998). Systematic gain-of-function genetics in *Drosophila*. *Development* **125**, 1049-1057.
Schimmelpfeng, K., Gogel, S. and Klambt, C. (2001). The function of leak and kuzbanian during growth cone and cell migration. *Mech. Dev.* **106**, 25-36.
Schindelholz, B., Knirr, M., Warrior, R. and Zinn, K. (2001). Regulation of CNS and motor axon guidance in *Drosophila* by the receptor tyrosine phosphatase DPTP52F. *Development* **128**, 4371-4382.
Schmid, A., Chiba, A. and Doe, C. Q. (1999). Clonal analysis of *Drosophila* embryonic neuroblasts: neural cell types, axon projections and muscle targets. *Development* **126**, 4653-4689.
Sekine-Aizawa, Y., Hama, E., Watanabe, K., Tsubuki, S., Kanai-Azuma, M., Kanai, Y., Arai, H., Aizawa, H., Iwata, N. and Saido, T. C. (2001). Matrix metalloproteinase (MMP) system in brain: identification and characterization of brain-specific MMP highly expressed in cerebellum. *Eur. J. Neurosci.* **13**, 935-948.
Sepp, K. J., Schulte, J. and Auld, V. J. (2000). Developmental dynamics of peripheral glia in Drosophila melanogaster. *Glia* **30**, 122-133.
Sepp, K. J., Schulte, J. and Auld, V. J. (2001). Peripheral glia direct axon guidance across the CNS/PNS transition zone. *Dev. Biol.* **238**, 47-63.
Serpe, M. and O'Connor, M. B. (2006). The metalloprotease tolloid-related and its TGF-beta-like substrate Dawdle regulate *Drosophila* motoneuron axon guidance. *Development* **133**, 4969-4979.
Shubayev, V. I. and Myers, R. R. (2004). Matrix metalloproteinase-9 promotes nerve growth factor-induced neurite elongation but not new sprout formation in vitro. *J. Neurosci. Res.* **77**, 229-239.
Siebert, H., Dippel, N., Mader, M., Weber, F. and Bruck, W. (2001). Matrix metalloproteinase expression and inhibition after sciatic nerve axotomy. *J. Neuropathol. Exp. Neurol.* **60**, 85-93.
Sink, H. and Whitington, P. M. (1991). Location and connectivity of abdominal motoneurons in the embryo and larva of Drosophila melanogaster. *J. Neurobiol.* **22**, 298-311.
Sink, H., Rehm, E. J., Richstone, L., Bulls, Y. M. and Goodman, C. S. (2001). sidestep encodes a target-derived attractant essential for motor axon guidance in Drosophila. *Cell* **105**, 57-67.
Steigemann, P., Molitor, A., Fellert, S., Jackle, H. and Vorbruggen, G. (2004). Heparan sulfate proteoglycan syndecan promotes axonal and myotube guidance by slit/robo signaling. *Curr. Biol.* **14**, 225-230.

Sternlicht, M. D. and Werb, Z. (2001). How matrix metalloproteinases regulate cell behavior. *Annu. Rev. Cell Dev. Biol.* **17**, 463-516.
Stickens, D., Behonick, D. J., Ortega, N., Heyer, B., Hartenstein, B., Yu, Y., Fosang, A. J., Schorpp-Kistner, M., Angel, P. and Werb, Z. (2004). Altered endochondral bone development in matrix metalloproteinase 13-deficient mice. *Development* **131**, 5883-5895.
Terman, J. R. and Kolodkin, A. L. (2004). Nervy links protein kinase a to plexin-mediated semaphorin repulsion. *Science* **303**, 1204-1207.
Terman, J. R., Mao, T., Pasterkamp, R. J., Yu, H. H. and Kolodkin, A. L. (2002). MICALs, a family of conserved flavoprotein oxidoreductases, function in plexin-mediated axonal repulsion. *Cell* **109**, 887-900.
Thor, S. and Thomas, J. B. (1997). The Drosophila islet gene governs axon pathfinding and neurotransmitter identity. *Neuron* **18**, 397-409.
Toba, G., Ohsako, T., Miyata, N., Ohtsuka, T., Seong, K. H. and Aigaki, T. (1999). The gene search system. A method for efficient detection and rapid molecular identification of genes in Drosophila melanogaster. *Genetics* **151**, 725-737.
Van Vactor, D., Sink, H., Fambrough, D., Tsoo, R. and Goodman, C. S. (1993). Genes that control neuromuscular specificity in Drosophila. *Cell* **73**, 1137-1153.
Viquez, N. M., Li, C. R., Wairkar, Y. P. and DiAntonio, A. (2006). The B′ protein phosphatase 2A regulatory subunit well-rounded regulates synaptic growth and cytoskeletal stability at the Drosophila neuromuscular junction. *J. Neurosci.* **26**, 9293-9303.
Wei, S., Xie, Z., Filenova, E. and Brew, K. (2003). Drosophila TIMP is a potent inhibitor of MMPs and TACE: similarities in structure and function to TIMP-3. *Biochemistry* **42**, 12200-12207.
Winberg, M. L., Mitchell, K. J. and Goodman, C. S. (1998a). Genetic analysis of the mechanisms controlling target selection: complementary and combinatorial functions of netrins, semaphorins, and IgCAMs. *Cell* **93**, 581-591.
Winberg, M. L., Noordermeer, J. N., Tamagnone, L., Comoglio, P. M., Spriggs, M. K., Tessier-Lavigne, M. and Goodman, C. S. (1998b). Plexin A is a neuronal semaphorin receptor that controls axon guidance. *Cell* **95**, 903-916.
Xiong, W. C., Okano, H., Patel, N. H., Blendy, J. A. and Montell, C. (1994). repo encodes a glial-specific homeo domain protein required in the Drosophila nervous system. *Genes Dev.* **8**, 981-994.
Yao, K. M. and White, K. (1994). Neural specificity of elav expression: defining a Drosophila promoter for directing expression to the nervous system. *J. Neurochem.* **63**, 41-51.
Yong, V. W. (2005). Metalloproteinases: mediators of pathology and regeneration in the CNS. *Nat. Rev. Neurosci.* **6**, 931-944.
Yong, V. W., Krekoski, C. A., Forsyth, P. A., Bell, R. and Edwards, D. R. (1998). Matrix metalloproteinases and diseases of the CNS. *Trends Neurosci.* **21**, 75-80.
Yong, V. W., Power, C., Forsyth, P. and Edwards, D. R. (2001). Metalloproteinases in biology and pathology of the nervous system. *Nat. Rev. Neurosci.* **2**, 502-511.
Yu, H. H., Araj, H. H., Ralls, S. A. and Kolodkin, A. L. (1998). The transmembrane Semaphorin Sema I is required in Drosophila for embryonic motor and CNS axon guidance. *Neuron* **20**, 207-220.
Yu, H. H., Huang, A. S. and Kolodkin, A. L. (2000). Semaphorin-1a acts in concert with the cell adhesion molecules fasciclin II and connectin to regulate axon fasciculation in Drosophila. *Genetics* **156**, 723-731.
Zhang, S., Dailey, G. M., Kwan, E., Glasheen, B. M., Sroga, G. E. and Page-McCaw, A. (2006). An MMP liberates the Ninjurin A ectodomain to signal a loss of cell adhesion. *Genes Dev.* **20**, 1899-1910.
Zuo, J., Ferguson, T. A., Hernandez, Y. J., Stetler-Stevenson, W. G. and Muir, D. (1998). Neuronal matrix metalloproteinase-2 degrades and inactivates a neurite-inhibiting chondroitin sulfate proteoglycan. *J. Neurosci.* **18**, 5203-5211.